Addis Ababa University

Addis Ababa Institute of Technology

School of Electrical and Computer Engineering

Design of Fuzzy Sliding Mode Controller for Heartbeat Pacemaker Based on ECG Signal Tracking

A Thesis Submitted to the School of Graduate Studies of Addis Ababa University in Partial Fulfillment of the Requirements for the Degree of Masters of Science in Electrical Control Engineering

By Anteneh Nebyu

Thesis Advisor: Dr. Dereje Shiferaw

November 2020

Addis Ababa, Ethiopia

Addis Ababa University

Addis Ababa Institute of Technology

School of Electrical and Computer Engineering

Design of Fuzzy Sliding Mode Controller for Heartbeat Pacemaker Based on ECG Signal Tracking

By Anteneh Nebyu

Approved by Board Examiners

Dr. Dereje Shiferaw	School of ECE Thesis Advisor	Signature	Date
Dr. Mengesha Mamo	School of ECE External Examiner	Signature	Date
Bethlehem Aberra	School of ECE Internal Examiner	Signature	Date
Dr. Yalemzewd Negash	School of ECE Dean	Signature	Date

Declaration

I, Anteneh Nebyu, declare that this thesis is my original work, has not been presented for a degree or any other qualification in this or other university.

…………………………
Anteneh Nebyu

Acknowledgments

First of all, praise and thank to Almighty God for his blessing and grace. Secondly, my deep gratitude goes to my thesis advisor, Dr. Dereje Shiferaw, for his valuable comments, suggestions and guidance, who helped me to complete the thesis work in this pandemic period.

Next, I am highly grateful to Control Engineering staffs Dr. Mengesha Mamo, Dr. Libsework Negash and Dr. Dereje Shiferaw for their commitment in arranging progress report monthly which was too useful. And, I would also like to thank Debre Markos University for the financial support.

I want to express my grateful appreciation to my wife, Bossena A., for her love, support, encouragement, and everything else.

Finally, I want to acknowledge my friend, Mequanent Argaw, for his support during documentation and my post graduate classmates for their idea support during the work.

Abstract

Every year, heart disease is becoming the major cause of death. Therefore, the need arises to find advanced approaches to keep the patients safety. Implantable cardiac pacemakers are an electronic device that can track and boost the heart rate and manage rhythm disorders.

This thesis presents nonlinear control of heartbeat model. Because of certain severe cardiac arrhythmias display nonlinear feature which is usually correlated with unpredictable and oscillatory behavior, a nonlinear technique is used to model heart electrical activity. Zeeman's heartbeat model was used to generate ECG signals. Existing model of heartbeat was analyzed and revised by integrating the control input to add the control mechanisms as a pacemaker.

In this study, sliding mode control (SMC) is applied to heartbeat model in order to track and generate real ECG signal. Fuzzy logic algorithm was also used with SMC to reduce chattering happened due to high frequency oscillations around the sliding surface that will shorten the life span of pacemaker. Therefore, a fuzzy sliding mode controller (FSMC) for cardiac pacemaker based on ECG signal reference tracking system was designed. In addition, since the heartbeat pacemaker is disturbed by the brain signal and sensor output delay, the robustness of the system to disturbance, parameter variations and possible time delay on the feedback system were analyzed.

The effectiveness of the proposed method was verified through simulation studies using Matlab/ Simulink software. The proposed control law has shown satisfactory performance in terms of tracking ECG signal of the actual data, obtained from the MIT- Boston's Beth Israel Hospital (BIH), and the physioNet database by eliminating chattering compared with the use of SMC controller. In addition, the result of root mean square error was reduced by 0.00005 % and total harmonic distortion analyzed from FFT window was reduced by 121.35 % when FSMC was applied to the system compared with SMC. The control strategy was also found to be robust with respect to external disturbances, parameter variations and random feedback delay. Therefore, control algorithm will be applied in dual sensor cardiac pacemakers for clinical use.

Key words: *Fuzzy sliding mode control, Electrocardiogram, nonlinear heartbeat model, phase portrait analysis, time delay, disturbance*

Table of Contents

List of Figures

List of Tables

List of Abbreviations

ANS	Automatic nervous system
AV	Atrioventricular
BBO	Biogeography based optimization
BPM	Beat per minute
ECG	Electrocardiogram
EEG	Electroencephalogram
ELC	Emotional learning control
EMG	Electromyography
ETDF	Extended time delay feedback
FPID	Fuzzy proportional integral derivative
FFT	Fast Fourier transforms
FSMC	Fuzzy sliding mode controller
HP	His purkinjie
HRV	Heart rate variability
MF SMC	Model free sliding mode controller
MPC	Model predictive controller
ODE	Ordinary differential equation
PID	Proportional integral derivative
RMS	root mean square
SA	Sino atrial
SMC	Sliding mode controller
VDP	Van der pol
WHO	World health organization

Chapter 1

Introduction

1.1. Background

Heart is a complex and most important part of human body [1]. Heartbeat is generated by firing pulse of the Sino-Atrial (SA) node, the natural pacemaker of the healthy heart [2]. This electrical pulse then propagates through the atria to ventricles via the atrioventricular node (AV) and the His-Purkinje system (HP), resulting in the cardiac muscle contraction and relaxation sequence. One of the most significant signals concerning to the operation of human heart is ECG signal. It is a time varying signal which represents the electrical potential generated in the cardiac muscle by electrical activity. A single ECG cycle is the reflection of contraction and heart relaxation which leads to pumping action of the heart. Characteristic information obtained from ECG could be used to indicate cardiac health and identify possible heart problems [3].

Recently, cardiovascular disease is major public health issue around the world. Around 9 % of all deaths in Ethiopia in 2012 were caused by cardiovascular disease according to World Health Organization (WHO) estimation [4].

In specific, the risk of sudden cardiac arrest, which is the cessation of typical circulation of the blood due to disruptions of the heart to contract successfully, which strikes individuals to death without any forebode, whether or not they have analyzed heart condition [5][6]. Thus, to avoid the accidental patients' death, early and exact determination and medical therapeutic treatment of heart disease is very vital [7]. Regular rhythm of heart is synchronized by normal pacemaker of heart, SA node. In the event that there is any issue in conduction system of heart and drugs are not effective, implantable devices are suggested.

Cardiac pacemakers have become a therapeutic apparatus used around the world with more than 250,000 pacemaker inserts each year [8]. It is a device that produces electrical stimuli and conveys them to the muscles of the heart, in the way as to cause the muscle to contract and the heart to beat [5]. One of the treatments to recover a victim's rhythm is to deliver the electrical pulse, which is well demonstrated as the most effective treatment for cardiac arrest [35].

Basically, it comprises of a pulse generator with rechargeable battery and lead connectors. The pacemaker's battery is usually made of lithium iodine, which gives a life span up to 10 to 12 years [9]. The heart rate and/or beat are checked by the electrocardiogram detector within integrated circuit of pacemaker to apply electrical simulations of the pulse generator to the myocardium through pacing leads if irregular heart beating is identified [7].

However, estimating the patient's body status, e.g., resting or walking conditions, is clinically required to alter the pacing rate to supply satisfactory cardiac output. Hence, numerous types of body sensors such as metabolic sensor and dual sensors have been connected in pacemakers to identify physiological changes of the body during possible daily activities [6]. In any case, dual-sensor pacemakers still require solid and advanced control strategies that help the heart beating to be more typical and steady than current rate-adaptive pacing systems [6] [7][9].

1.2. Problem Description

Aging or heart diseases disturb the capacity of the SA node, or the electrical conduction paths may be disrupted to correctly pace a heart's rhythm, resulting in slower, quicker, or stopped beats. Such forms of heart disorders are now being treated by implantable artificial cardiac pacemakers utilizing electric simulation to synchronize the heart as near to the normal heart rhythm as possible.

Recent wireless pacemakers are highly attacked in their sensor outputs due to magnetic interference. Therefore, the shocking signal delivered to heart muscles may be delayed or missed in order to bring normal beating [23] while using conventional linear controllers, like PID control, which leads a patient to a sudden death. Example, it often wrongly adds shocking voltages of 600 to 700 to the heart even if no blockage, which is too risky [10].

In addition, since some abnormal heartbeats (arrhythmias) produce chaotic like response which is exhibiting nonlinearity property and the heart rate is also affected by the instructions fired from the brain signal, the control mechanism should be nonlinear and robust against such undesired physiological complications and disturbance of heartbeat.

Mean that pacemaker efficiency depends on both sensors and controller outputs [11]. Sliding mode controller is a fast tracking and robust under uncertain, time delayed and disturbed systems. Therefore, this research work presented fuzzy sliding mode controller for dual sensor cardiac pacemaker based on ECG signal tracking. Sliding mode along with fuzzy logic algorithm was used to eliminate chattering.

1.3. Objectives of the Thesis

1.3.1. General Objective

The general objective of a system is to design and simulate fuzzy sliding mode controller for cardiac pacemaker based on ECG signal tracking.

1.3.2. Specific Objectives

- To study the electrical conductivity behavior of heart and its mathematical modeling.
- To analyze the validity of heartbeat model.
- To design a controller that can track and generate synthetic ECG signal based on actual reference data, obtained from physioNet database.
- To apply fuzzy logic algorithm to develop the performance of dual sensor cardiac pacemaker by reducing chattering.
- To simulate and test the overall system using MATLAB/Simulink.

1.4. Contribution of the Thesis

The application of sliding mode controller with fuzzy logic algorithm to Zeeman nonlinear heartbeat dynamic was introduced. The control algorithm used has better performance in the presence of disturbance of heartbeat and time delay attack in the sensing system.

1.5. Scope of the Thesis

The thesis covers the design and simulation of fuzzy sliding mode controller for dual sensor cardiac pacemaker based on ECG data tracking. Here, the patient was assumed to be at rest condition. So, the activity state in dual senor is zero.

The brain signals disturb heartbeat electrical activity. In this thesis, the signals triggered from parasympathetic nervous system to decrease the heart rate during rest condition were not considered. But, the sympathetic signal simulation causing to increase the heart rate due to anxiety or disease was considered as a disturbance. Physiological complications that delay the electrical propagation was also not considered.

1.6. Methodology

The following approaches were used to address the aforementioned problems.

- Reviewing Literature: previous studies and journal papers related to design and development of pacemaker controller were reviewed and different concepts adopted.
- Collecting Data: the existing secondary data sources of heart have been collected. Several mathematical models of heartbeat system were also studied.
- Controller Design: sliding mode controller along with fuzzy logic was designed as pacemaker to track the actual ECG signal. Integration of the whole system with controllers has been carried out.
- Simulation: the developed system was simulated by MATLAB/SIMULINK
- Controller Testing: the robustness of the system was tested in response to external disturbance, fast tracking under parameter variations and time delay attack in the sensed system to generate and track ECG signal were demonstrated.
- Finally, results, discussions and conclusions were demonstrated

1.7. Organization of the Thesis

This thesis is organized into five chapters. The first chapter introduces the heartbeat system and pacemaker, problem statement and objectives as well as contribution of the thesis.

In chapter 2, the review of human heart and cardiac disease, sensing system and types of pacemakers, and different related works for pacemaker controllers are presented. Heartbeat model analysis, validation, considered disturbance and heart rate calculations are conducted in chapter three. The application of sliding mode control theory to heartbeat system by introducing fuzzy logic algorithm to eliminate undesirable chattering happened in pacemaker signal is also studied in chapter 3.

Simulation results and discussions are presented in chapter four. Finally, chapter five presents conclusions and future works.

Chapter 2

Human Heart and Cardiac Diseases

2.1. The Heart and Circulatory System

A human heart shown in figure 2.1 is a myogenic muscular organ with a circulatory mechanism that induces regular rhythm contractions to circulate blood into the blood vessels. It has two different pumps: a right heart pumping oxygen into the lungs, and left heart pumping blood into the peripheral organs. In addition, the part of heart is a two chamber pulsative pump including atrium and ventricle. Atrium is a weak priming pump that helps to move blood into the ventricle. The ventricles also supply the major pumping action which either propels the blood into the pulmonary circulation via the right ventricles or the left ventricle's peripheral circulation [12].

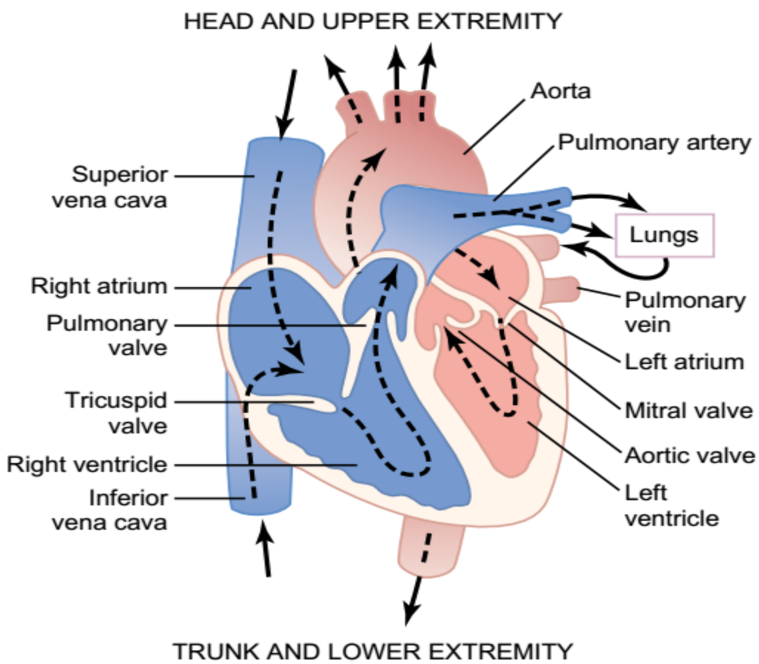

Figure 2.1: Structure of the heart [12]

2.2. Electrical Conduction System of Heart

The heart is made up of atrial and ventricle muscles which make up the myocardium and specific fibers which can be subdivided into fibers of excitation and conduction. When electrical signal is activated, muscle contraction occurs [6].

The SA node activation in atria, introducing a synchronized contraction of the atrial walls. The impulse, then, enters into the AV node, the only electrical path between the atria and the ventricles. The AV node provides an important delay, which enables the atria to complete contraction before ventricular contraction is triggered. This interval ensures optimal ventricular filling. Subsequently, the His-Purkinje system, containing the bundle of His, bundle branches, and Purkinje fibers, perform the electrical impulse at high level. If His bundle is triggered, the impulse divides into the right bundle, leading to the right ventricle, and left bundle divisions serving the left ventricle. The purkinjie fibers distribute the excitation across the two ventricles, enabling a synchronized and large contraction [12]. The electrical conduction system is shown in figure (2.2) below.

In regular sinus movement, the SA node has the greatest influence over the heart intrinsic rate of 60-100 bpm, depending on the hemodynamic demand. AV nodal cell has an intrinsic intensity of around 50 beats per minute (bpm). While Purkinje fibers depolarize at a pace of not more than 40 bpm.

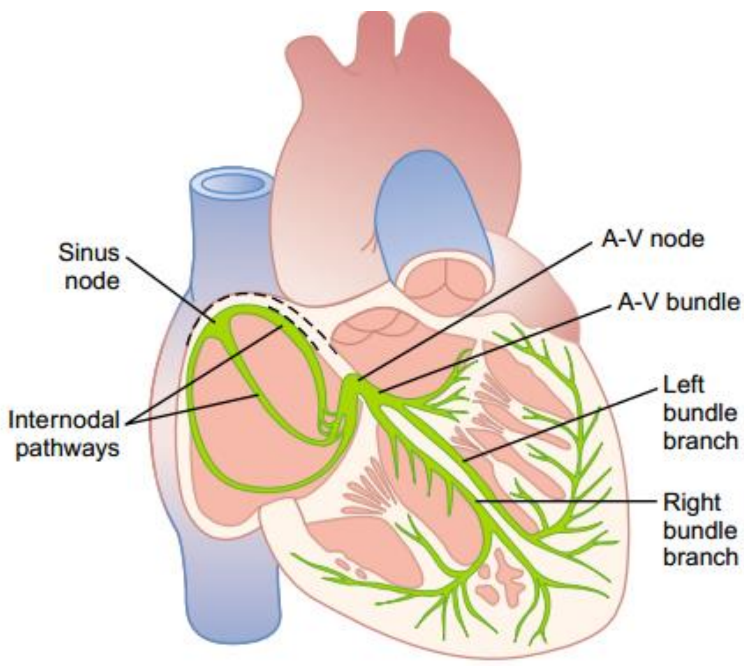

Figure 2.2: Cardiac conduction system [12]

2.3. Diastole and Systole Periods

The terms diastole and systole correspond to relaxation and contraction of heart muscles, respectively.

The heart fills all body organs and tissues with oxygenated blood. During this interval the relaxing stage is called diastole and the contraction stage is called systole. Figure (2.3) indicates the numerous activities to the left part of heart during the cardiac process. The top three curves reflect variations in pressure in aorta, left ventricle, and left atrium, respectively. The fourth plot indicates the shifts in the ventricular pressure, the fifth is electrocardiogram and the six is the phonocardiogram which is a measurement of the sounds made by the heart, primarily by the heart valves when it pumps [12].

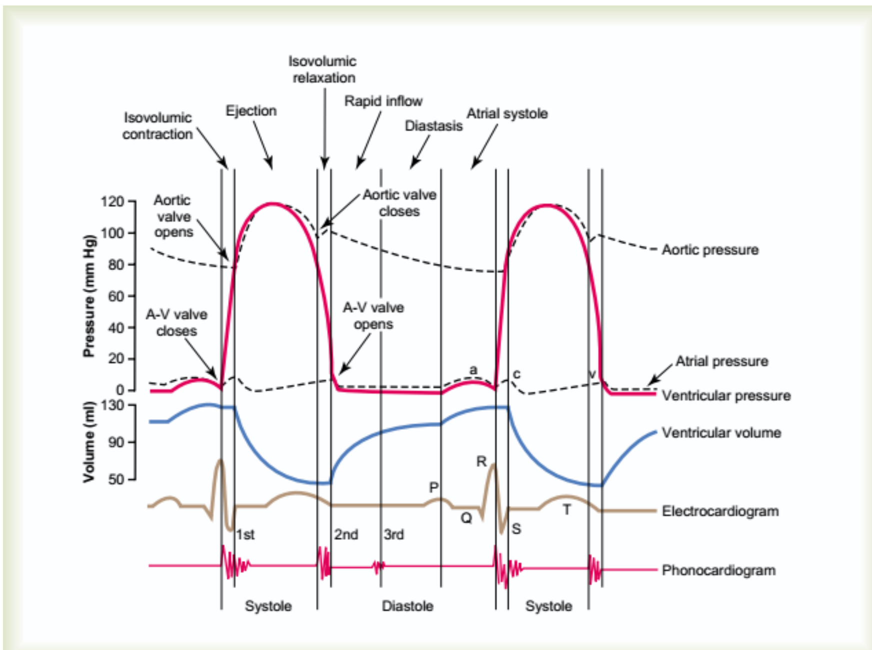

Figure 2.3: Cardiac cycle events for left ventricular function [12]

2.3.1. Electrocardiogram (ECG)

Through a microelectrode, which is implanted into a cardiac muscle cell, cardiac electrical impulses may be captured at an intracellular stage. In addition, the electrical potential produced by cardiac electrical activity may be recorded on the thorax surface. The ECG is a test of the heart muscle tissue's extracellular electrical activity. A very complicated process is provided by the transmission wave front of the cardiac electrical signal across the body. Several cardiac signal measurement devices have already suggested where leads are used to quantify possible variations on the body surface between points. In fact, the calculated signal is dipole projection along the line identified by the leads. Therefore, various measurements are obtained depending on the position of leads, but typically the signal includes the following waves [35]:

P-Wave: is the first wave reported in the ECG which reflects the activation of the atrium after the simulation of the sinus. In adult, it normally lasts between 60 and 90 ms, has a round shape with maximum amplitude of between 0.25 and 0.3 mV.

PR-Interval: is calculated from the beginning of P wave to the QRS complex beginning and lasts 90 ms.

QRS-Complex: it refers to the ventricular contraction and is determined from the beginning of the first wave (regardless of whether it is Q or R wave), to the final wave (R or S wave). The complex lasts around 80 ms in average and has a distinct outline owing to the elevated signal frequencies. Depending on the lead device used, its form differs a lot.

ST-Interval: it continues from the end of the QRS-complex until the beginning of the T wave and correlates to part of the ventricular repolarization.

T-Wave: this reflects ventricular simulation, has a circular configuration with amplitude of approximately 0.6 mV.

The ECG signal presented schematically in figure 2.4 consists of three waves, namely the P-wave (depolarization of atrial), R-waves (depolarization of the ventricles), and T-wave. By finding the correct R wave levels, the heart rate can be correctly measured and then recorded [7].

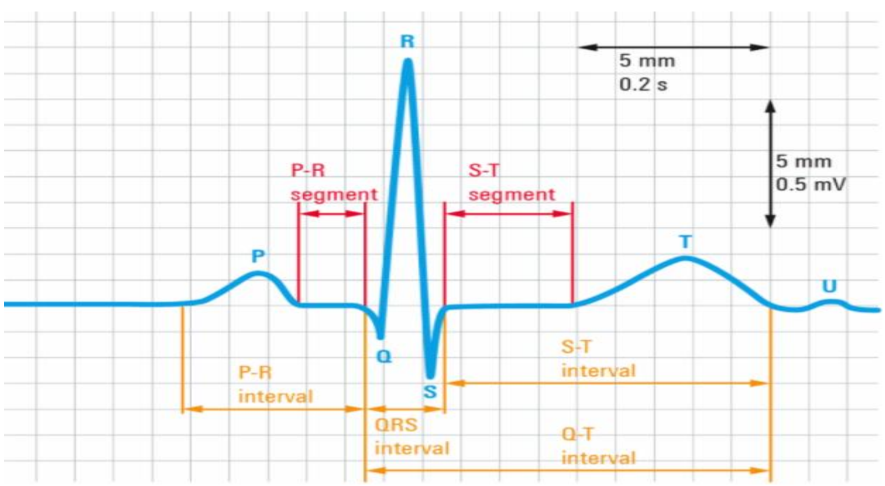

Figure 2.4: ECG waves and interval [11]

2.4. Cardiac Disease -- Arrhythmias

Arrhythmia is the disorder that arises from electrical heart rate disruption accompanied by an abnormal heart rate and irregular heart beating patterns. The origin of cardiac arrhythmias appears to be one or a combination of the following irregularities in the heart's rhythm conduction mechanism [12]:

1. Pacemaker irregular rhythmicity
2. Pacemaker move from the sinus node to a separate location in the heart
3. Blocks the transmission of the impulse through the heart at various points
4. Abnormal impulse delivery paths via the heart
5. Spontaneous generation of unwanted impulses in nearly every part of the heart

Coordinating the electrical function of the heart can be affected by the conduction defects and refractory properties in the cardiac tissue. This may be classified in to bradycardia, tachycardia and cardiac arrest.

A). Bradycardia

It may be due to impulse generation failure with abnormalities in the SA node, or impulse propagation dysfunction in which the conduction from the atria to the ventricle is interrupted or even blocked. This means a low heart rate can result in poor blood flow, typically described as less than 60 bpm as shown in figure (2.5) [12].

Figure 2.5: Sinus bradycardia [12]

B). Tachycardia

It means a rapid heartbeat and is typically described as more than 100 bpm in adult human. Figure (2.6) shows an electrocardiogram obtained from a patient with tachycardia. This electrocardiogram is regular except the heart rate is around 150 bpm instead of just the normal 72 bpm, as calculated by time difference between the QRS complexes. The general symptoms of tachycardia include raised body temperature, cardiac activation by sympathetic nerves, or cardiac toxicity [12].

Figure 2.6: Sinus tachycardia [12]

C). Atrial Fibrillation

In figure 2.7 is a form of erratic heart rhythm, typically of very rapid heart rate. During atrial fibrillation, the electrical activity becomes erratic, triggering abnormal and fast rhythm that the blood cannot be properly circulated through the body (Charles Patrick, 2020).

Figure 2.7: Atrial Fibrillation [12]

D). Ventricular fibrillation (VFiB)

It is a form of pathological heart rhythm in which the heart rate is irregular and typically fast due to excessive contractions in the lower cardiac ventricles chambers. VFiB happens when the electrical signals inside the ventricular muscle tissue becomes chaotic, resulting in no effective rhythm (Charles Patric and Jerry R.balentine). During VFiB, the heart quivers and pumps little or no blood to the body. If not treated immediately, it can induce unexpected heart arrest if not adequately managed.

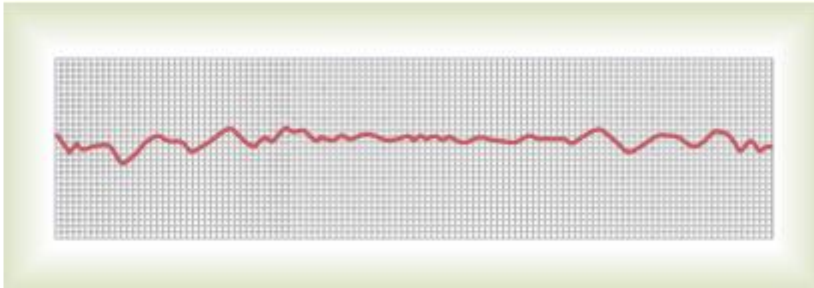

Figure 2.8: Ventricular Fibrillation [12]

2.5. Heart Rate Variability

The reciprocal of the RR interval is heart rate which has a strong effect on blood pressure. The autonomic nervous system (ANS) is responsible for regulating the blood pressure. The decision for automatic function takes place in the medulla of the hypothalamus and the brain stem. Instructions are transmitted from these centers through nerves that link the brain to the heart. There are two major nerve sets that represent the parasympathetic and sympathetic types of ANS, all of which innervate the heart. The heart rate may be increased through sympathetic activity and reduced through parasympathetic (vagal) activity [14]. The SA node has an intrinsic heart rate, but this is usually modified by the central nervous system, namely, the automatic nervous system (ANS).

At stressful period the sympathetic nervous system is triggered. It raises the rate of SA node firing (hence raises heart rate) and also innervates the myocardium itself, raising the rate of propagation of depolarization wave, primarily through the AV node, and raising the force of mechanical contractions [13].

2.6. Sensing System and Heart Pacemaker

A pacemaker is a device that produces electrical signal and sends them to the heart muscles (myocardium) to contract and relax. It is used to treat rhythms of the heart that are too sluggish, too fast or some other irregularity. Figure 2.9 illustrates how a pacemaker is inserted in a human body. A pacemaker is allowing an irregular heart rhythm to regain a more active lifestyle. In the event of deadly cardiac irregularities, the pacemaker must be calibrated to produce compulsive, fast pulse that returns irregular to normal rhythm [7].

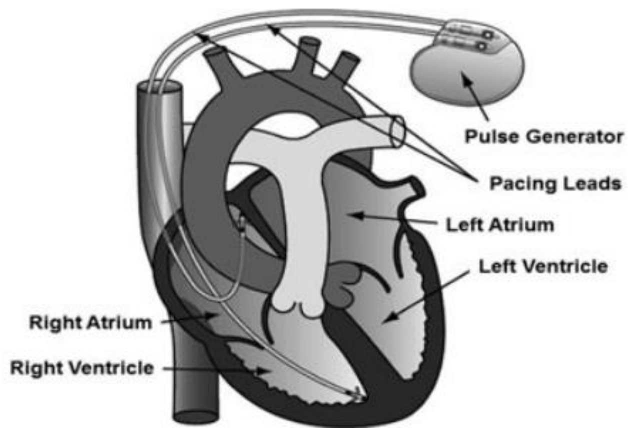

Figure 2.9: Schematic view of the heart with implantable pacemaker [9]

2.7. The History and Development of Cardiac Pacemaker

The following are the overview of the pacemaker's history and growth.

2.7.1. Artificial Pacemakers

An artificial pacemaker is a tool that provides the heart muscle with a regulated, rhythmic electrical simulation to sustain an efficient heart rhythm for long period of time, maintaining efficient hemodynamic efficiency functionality [15]. A pacemaker consists of three parts: an electrical pulse generator, a power source (battery) and an electrode (lead) system, as shown in figure 2.10.

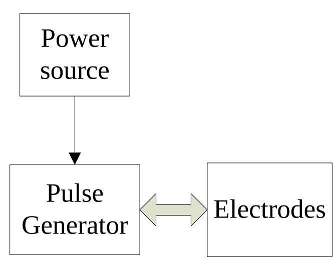

Figure 2.10: Basic pacemaker functional block diagram [15].

2.7.2. Implantable Pacemakers

In 1959, the first pacemaker which was completely implantable was developed. The system was used mainly to treat patients with a full block of AV caused by Stokes Adams diseases, resulting in a single chamber ventricular pacing. Its diameter is 6 cm and 1.5 cm in thickness, and the pacemaker's total weight was around 180 g. The pacemaker circuit supplied the electrode with 1 ms long pulses, a pulse amplitude of 10 mA, and a repeat rate of 60 bpm. Under these conditions, the average current drain of the circuit was about 12 μA, which, energized by ten mercury-zinc cells, provided an approximate continuous operating life of five years [15]. Figure 2.11 shows first implanted pacemaker's schematic.

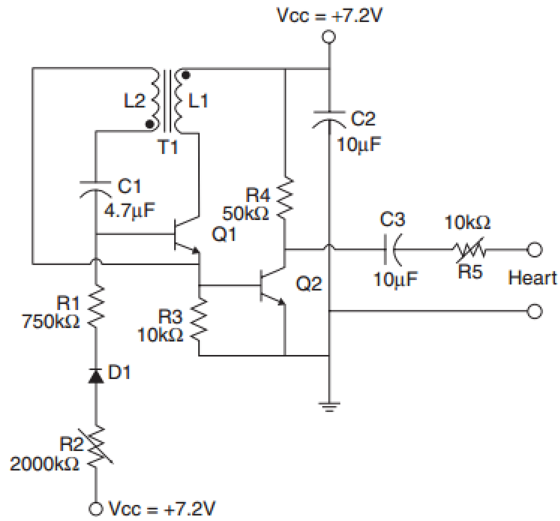

Figure 2.11: A schematic of the first implanted pacemaker [15]

2.7.3. Demand Pacemakers

The early pacing system merely transmitted a fixed pulse rate at a predetermined rhythm to the ventricle, regardless of any random cardiac operations. Such pacemakers, named intermittent or fixed rate pacemakers, interfere with the normal operation of the heart and may often also induce arrhythmias or ventricular fibrillation (VF). Through attaching a sensing amplification to the asynchronous pacemaker to sense endogenous cardiac activity and thereby escape this interference, a demand pacemaker generates electrical impulse for simulating the heart even in the absence of normal heartbeat. The demand pacemaker's other benefit over the fixed rate device is the machine's battery life is extended, because it is only triggered while pacing inputs are required. Berkov presented the idea of demand in June 1964, which is the foundation of all current pacemakers and the schematic is shown in figure 2.12 [15].

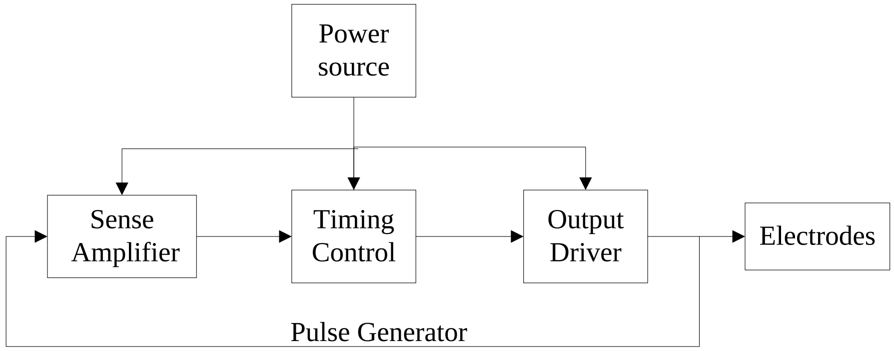

Figure 2.12: Basic demand pacemaker functional block diagram [15]

2.7.4. Dual Chamber Pacemakers

Usually, a dual chamber pacemaker needs two pacing leads: the right atrium, and the right ventricle. A dual camber pacemaker tracks and senses electrical activity in the atrium and /or ventricle if pacing is required. When pacing is required, the atrium and /or ventricle pacing pulses are synchronized to replicate the normal way. It was launched in the 1970. In 1971, Berkovits provided one of the first dual chamber pacemaker and reported a bifocal (AV) pacer that only sensed in the ventricle but controlled all chambers. The bifocal pacemaker may offer stimulation to the atrium and then, after a sufficient time, to the ventricle in the case of an atrial fibrillation or a sinus node syndrome plus AV block [15]. A schematic design of the system is shown in figure 2.13.

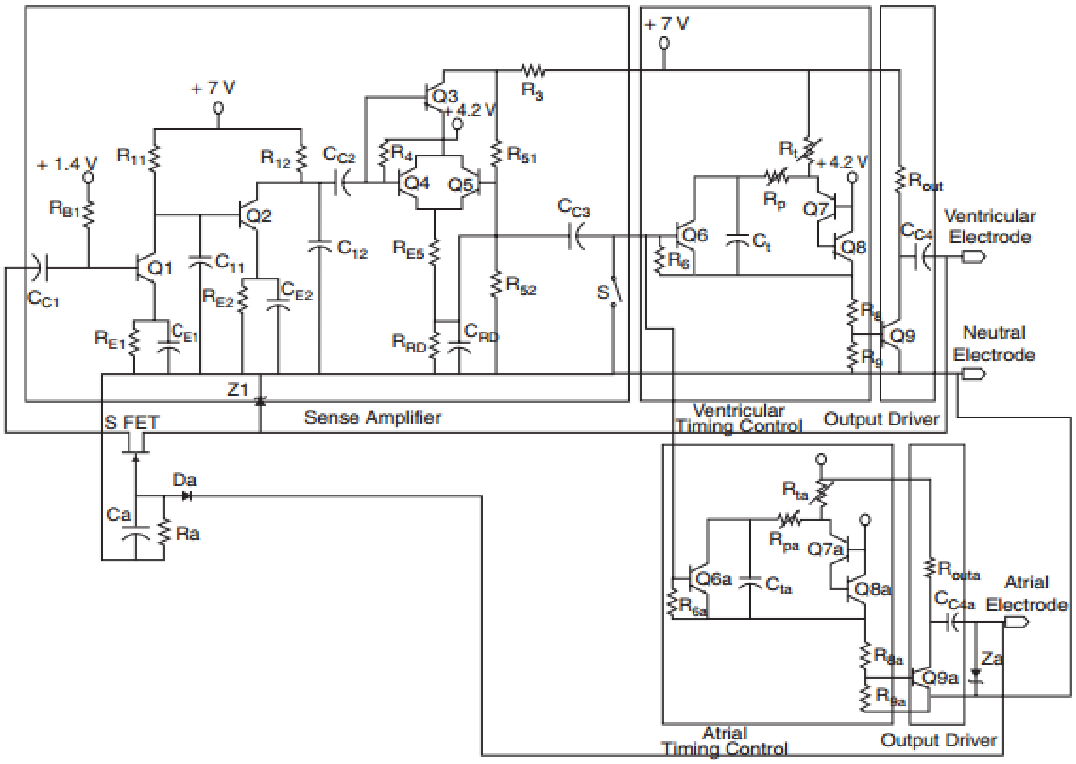

Figure 2.13: Schematic of the dual-chamber demand pacemaker [15]

2.7.5. Rate Responsive Pacemakers

The new developments in the early 1980’s include the creation of rate responsive pacemaker, which could control their rate of pacing based on the performance of a sensor device embedded in the pacemaker. A sensor system consists of a mechanism to calculate the specific body parameters (e.g. body position, respiration rate, PH, and blood pressure) and a pacemaker algorithm that can change the output of the pacemaker according to the calculated quantity.

Current rate-responsive pacemakers are able to respond to a board variety of sensor details about the patient’s medical conditions and/or physical activity. The machine is based on pacemaker providing a generator of demand pulses and is adaptive to the parameter calculated [15]. A rate responsive pacemaker block diagram is shown in figure 2.14.

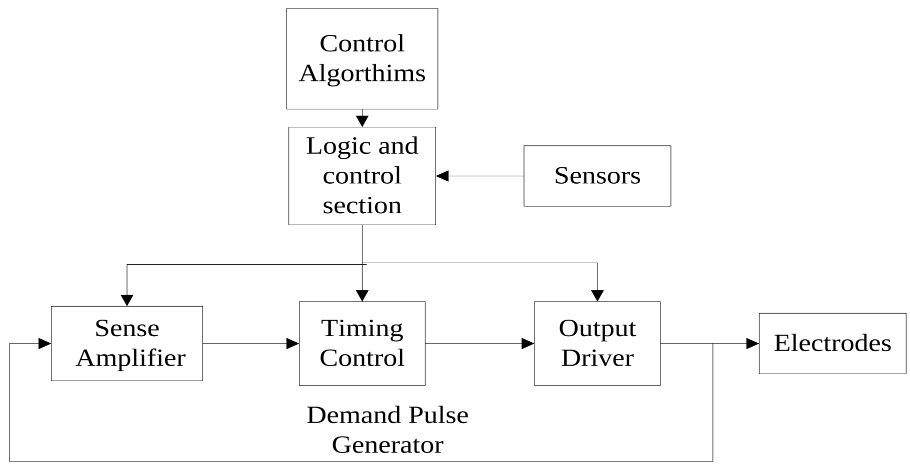

Figure 2.14: A block diagram of a rate-responsive pacemaker [15].

2.8. Biosensors in Pacemaker System

A body sensor is a sensing system that integrates a biological portion with a physiochemical part of detector. Implantable sensors measure parameters within the body and act mainly as interfaces to a very small software programs connected or inserted into human bodies.

Biosensors are used to detect body motion by responding to acceleration (accelerometer) and calculate the degree of physiological change through exercise or other circumstances (QT interval). Table 2.1 [5] [6] explains the sensor types for the pacemaker systems.

Table 2.1: Features of main Biosensors

Activity sensor (Accelerometer)	Minute ventilation	QT interval	Dual sensors
Body movement or vibrations	Volume of air inhaled/ exhaled in one minute	Intervals in pacing spike and T-wave	Dependent on two self-sensing devices
Rapid response to exercise	Physiological correlated with metabolic demand	Important ECG diagnostic parameter	Control each other
Less physiologically accurate	Slow respond to exercise	Unstable chronically	High power consumption

2.8.1. Dual Sensors

Dual sensors are used to prevent excessive rate fluctuations to have more precise diagnostic data analysis such that two sensors can account for each other. Both sensors will monitor each other during cross check, and the rate of pacing can only be adjusted if both or a prevailing sensor agrees [5] [6].

2.8.1.1 Activity Sensor

Activity sensors are old and widely used, which offer a rapid response to exercise by evaluating body vibrations or moves. An accelerometer detects the postural changes and the physical activity related to body motions. Usage of an accelerometer to track body movement is easy yet reliable method for action sensing.

As it is noninvasive (the sensing system is mounted inside the pacemaker without physical interactions with body), it is the chosen strategy used in most rate responsive pacemakers [15] [17] [18]. Schematic description of how an activity sensor is represented using a pulse generator positioned with accelerometer is shown in figure 2.15.

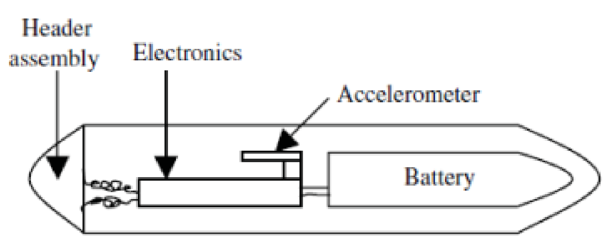

Figure 2.15: Activity sensing system [18]

2.8.1.2. QT Interval Sensor

It is a form of metabolic sensor that measures the actual heart rate values. QT length in the ECG represents contraction to relaxation of ventricle [6] [18]. Long QT intervals on the ECG are associated with an increased risk of arrhythmia and sudden death.

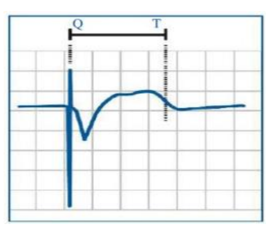

Figure 2.16: QT interval

2.9. Related Works

Several authors have designed the controller algorithms in recent years to get heartbeat to the desired level. They motivated the creation of reliable and quick responsive pacemakers. Some related works were reviewed.

W. V. Shi and M. C. Zhou presented a sample of the body sensors used in pacemakers, announced the latest technologies and innovations of contemporary pacemakers, and innovative body sensor varieties integrated in pacemakers with their reasoning, functionality and implementations. For tolerance of the heart rhythm, utilizing one sensor is not optimal and for optimum rate tolerance, integrating various kinds of sensors (dual sensors) is safer [6].

W.V. Shi and M. C. Zhou designed fuzzy PID controller for dual sensor pacing system for bradycardia patient at rest. The significance of this approach is that the target heart rate pattern tracked satisfactorily as the authors stated. New cardiac layout, sensor device, and comparative tests revealed the dominance of the FPID controller relative to fuzzy logic controller in obtaining a better correlation between natural heart rate and target profile. This model, though, has several disadvantages, such as 2.3-2.6 percent error levels. The authors obtained a low overshooting result with gradual time increase and time settlings [7].

H. Karam E. et. al. simulated model free sliding mode controller (MF-SMC) for heart rate pacemaker based on BBO algorithm. MF-SMC scheme was proposed to regulate heart rate of a pacemaker. Here the BBO algorithm was used to determine the optimum value of the controller parameter and thus improved the performance of the heart rate. The simulation result indicated that the boundary MF-SMC provides the better result compared with MF-SMC without boundary layer. A disturbance was also introduced to enhance the work of the proposed controller and the response was quick and perfect [19]. The authors in [7] and [8] used the heart model as a simple linear transfer function.

M. J. Lopez, et. al. simulated heart rhythm dynamic and control. It was implemented through proportional control law based on ECG signal reference tracking, and the control algorithm was tested for various cardiac pathologies. For simulation of cardiac rhythm dynamics, a mathematical model based on six differential equations with delay time was used. The result was noticed that the system, with very low error magnitude, returned the chaotic unpredictable rhythms to standard rhythm. In this case, the authors obtained the controller gain manually [20].

W. Thanom and R. N. Loh presented the implementation of the nonlinear control system principle focused on linearization of input output to biological heartbeat. Several cardiac based mathematical models were studied, and the author selected two models made by Zeeman. The heartbeat models are minimum phase system appropriate for the design of output tracking control laws; they were used to produce synthetic ECG signals using these output tracking control rules. The simulation results indicated that ECG data from the William Beaumont Hospitals and the PhysioNet database tracked satisfactorily [21] [26].

W. Thanom and R. N. Loh presented a nonlinear system control hypothesis focused on linearization of input output and an observer was introduced to estimate unknown variables. For this analysis, Zeeman models were selected because they not only explain the heartbeat but also have a clear biophysical connection to the complex variables with a minimum phase. The simulation findings revealed with asymptotic stable tracking error and the outputs of the system tracks the existing ECG data from the PhysioNet database [22].

Arman Sargolzaei, et. al. proposed the nonlinear heartbeat control under time delay switched feedback using emotional learning. The result indicted that the emotional learning control (ELC) implemented to Zeeman’s nonlinear heartbeat model can track the ECG signals. In addition, the ELC’s robustness to control heart model under time delay switch attack has been demonstrated in the sensing loop. It was also shown that ELC is more robust than other control methods like the classical PID and the predictive control model (MPC) [23].

B. B. Ferreira, et. al. proposed the application of an extended time delay feedback (ETDF) chaos control mechanism to a cardiac system developed as a three coupled oscillator, connected to time delay couplings. Estimating the ECG signals, cardiac behavior was analyzed and two different cases were viewed: normal and ventricular fibrillation linked with chaos becoming a critical abnormal behavior of the heart. The results indicated that applying the ETDF method is an integration way for avoiding critical behaviors such as ventricular fibrillation with very little control effort [24].

A new dynamic control system for the control of abnormal synthetic ECG signals has been introduced by **S. Behnia and J. Ziaei**. The authors proposed an approach to chaos control known as dynamic control to maintain normal signals, and the method of contrasting before and after control phase space diagrams was used. The analysis results indicated that the presented system was successful at implementing the heart to reassume a period of limitations [25]. Observer dependence algorithms in the authors [22], [23] and [24] for chaos control is a serious risk to heart health.

From the previous studies, the pacemakers' great difficulty is to develop an effective controller that tracks and generates ECG data with a near matched rate of pacing by eliminating abnormal rhythm correlated with cardiac pathologies. Observer dependence is, however, one of the key challenges of the methods mentioned in feasible applications.

In this study, fuzzy sliding mode controller for cardiac pacemaker is effective in tracking ECG signal in case of external disturbance and time delayed systems without using observer mechanisms.

Chapter 3

Analysis of Heartbeat Model and Methodology

3.1. Mathematical Model of Human Heart

Mathematical modeling of biological signal is very challenging and relatively new research work to be undertaken. This gives a better understanding of the underlying physical phenomena resulting in various physiological signals in the human body such as electrocardiogram (ECG), electroencephalogram (EEG), electromyography (EMG) etc. [16] [27]. These physiological signals are often used by physicians throughout the year to detect human organ abnormal behavior.

For the simulating electrical processes of human heart, complete or partial, linear or nonlinear models, various modeling approaches with different level of details have been proposed and utilized in order to generate various healthy and diseased ECG waves, in particular the chaotic responses. Some models generate real ECG data using a dynamical system of a heart [26] [28] [29] [30]. For others, the heart model is designed based on natural cardiac pacemakers [31] [32] [33] [34] [36] using various modifications of nonlinear relaxation oscillators specifically coupled van der pol oscillators.

3.1.1. Heartbeat Modeling using Dynamic System

The original paper [26] by Zeeman in 1972 studied two forms of excitable biological systems: nerves and heart. He developed electric neural simulation based on the van der pol linear equations with nonlinear coupled differential equations. Both models are focused on the pace making triggered by the Sino Atrial node, that is superior pacemaker compared to the Atrio-Ventricular (AV) junction's slower one. However, these models were not considered the sympathetic and parasympathetic modulations that are responsible for HRV generation [29]. The original Zeeman heartbeat model is described as:

$$\begin{aligned} \varepsilon\dot{x}_1 &= -\left(x_1^{\,3} - T x_1 + x_2 \right) \\ \dot{x}_2 &= x_1 - x_d \end{aligned} \tag{3.1}$$

Where, $x_1(t)$ defines the length of muscle fiber in heart; $x_2(t)$ is the variable related to electrochemical activity, and could be measured as membrane potential across muscle fiber, ECG signal; ε a small positive constant associated to the fast eigen values of the system; x_d is the average cardiac muscle fiber length during diastole (the duration of time when the blood is refilled by the heart contraction). $T > 0$ is the muscle tension and related to blood pressure.

In [30], the Zeeman's 2nd order heartbeat differential equations (ODE) has been updated by adding a switch (on/off) control variable showing the contraction and relaxation function of the pacemaker to the heart. It is described as:

$$\varepsilon\dot{x}_1 = -\left(x_1{}^3 - Tx_1 + x_2 \right)$$
$$\dot{x}_2 = (x_1 - x_d) + (x_d - x_s)\,\mathrm{u(t)},\ \mathrm{T} > 0 \tag{3.2}$$

Additional parameters, x_s represents typical length of muscle fiber during systolic state; *u(t)* the heart pacemaker control signal that guides the heart into diastole and systolic states.

Jafarnia. D. et. al. revised the 3rd order Zeeman nonlinear model by introducing control parameter which influences the oscillation frequency to regulate the HRV utilizing a neural network to produce ECG signal [32]. The 3rd order heartbeat is described as:

$$\varepsilon\dot{x}_1 = -\left(x_1{}^3 + x_1 x_2 + x_3 \right)$$
$$\dot{x}_2 = -2x_1 - 2x_2$$
$$\dot{x}_3 = -x_2 - 1 + \mathrm{u(t)} \tag{3.3}$$

Where, $x_1(t)$ represents the length of muscle fiber; $x_2(t)$ represents tension in muscle fiber; $x_3(t)$ related to electrochemical activities; *u(t)* describes the cardiac pacemaker control signal that guides the heart into diastole and systole states.

The model dynamics of 3rd order heartbeat system has no significant difference with the 2nd order system except tension in muscle fiber caused by blood pressure is considered as a state variable.

3.1.2. Heartbeat Modeling using Natural Pacemakers

Because of the qualitative characteristics of excitation potential of the heart are very similar to the classical Van der pol dynamics behavior [31], the oscillator can therefore be viewed as the starting point of modeling. The combined Van der pol (VdP) oscillator models at the AV node make it more involved in pace making [32]. The model helps one to understand the effort of the coupling of natural electrophysiological dynamics between SA and AV pacemakers [31].

HECS (Heart Electrical Conduction System) was found to be the coupled VdP oscillator in one of the earliest study by Van Der Pol and Van Der Mark in 1928 [32]. The ECG was not, however, produced.

$$\ddot{x} + \alpha\,(x^2 - \mu)\dot{x} + w^2 x = F(t) \tag{3.4}$$

Where, $\alpha > 0$ and $\mu = 1$ nonlinear dumping forces; W normal frequency of oscillator; *F(t)* external driving pulse; *x(t)* corresponds to the electrical heart pulse amplitude(action potential).

Then after, many studies have been developed to model the cardiac rhythms. A modification of the original Van der Pol oscillator was suggested Grudzinski and Zebrowski [34] to capture some significant aspects of the potential for heart activity represented by the natural pacemaker.

$$\ddot{x} + \alpha\,(x - v_1)(x - v_2)\dot{x} + \frac{x(x+d)(x+e)}{ed} = F(t) \tag{3.5}$$

Where, α modifies the pulse shape, which changes time that the heart receives the stimuli, v_1 and v_2 replaces the damping terms, e control the atrial or ventricular contraction period, d is parameter that arises when the harmonic forcing of classic equation is replaced by a cubic terms and $F(t)$ is an external forcing. Where, $v_1 v_2 < 0$. $d, e, a > 0$.

The model, further, was modified by Santos et al. [33], who presented a model of the cardiac dynamics composed of two coupled modified Van der Pol oscillators, representing the behavior of two pacemakers.

$$\dot{x_1} = x_2$$

$$\dot{x_2} = k\,(x_1 - w_1)(x_1 - w_2)x_2 - b_1 x_1 + c_1(x_3 - x_1) + a_1 \sin(w_1\,t)$$

$$\dot{x_3} = x_4$$

$$\dot{x_4} = k\,(x_3 - w_1)(x_3 - w_2)x_4 - b_2 x_3 + c_2(x_1 - x_3) \tag{3.6}$$

Where, the pairs (x_1, x_2) & (x_3, x_4) show SA and AV Oscillators, respectively, and K, w_1, w_2, b_1, b_2, c_1, c_2 represent model parameters.

Gois and Savi [35] simulated ECG signal via a mathematical model consisting of three updated Van der Pol oscillators, representing the Sino-Atrial(SA), Atrioventricular(AV) and the His-Purkinje mechanism, linked by time delay couplings. Numerical calculations were conducted to generate the ECG signal which could be changed by adjusting the parameters of the coupling.

$$\dot{x_1} = x_2$$

$$\dot{x_2} = -a_{SA}\, x_2\, (x_1 - w_{SA1})(x_1 - w_{SA2}) - \frac{x_1(x_1+d_{SA})(x_1+e_{SA})}{d_{SA}\, e_{SA}} + \rho_{SA} \sin(w_{SA}\ t) - k_{AV-SA}\, x_1 + k^t{}_{AV-SA}\, x_3{}^{\tau_{AV-SA}} - k_{HP-SA}\, x_1 + k^t{}_{HP-SA}\, x_5{}^{\tau_{HP-SA}}$$

$$\dot{x_3} = x_4$$

$$\dot{x_4} = -a_{AV}\, x_4\, (x_3 - w_{AV1})(x_3 - w_{AV2}) - \frac{x_3(x_3+d_{AV})(x_3+e_{AV})}{d_{AV} e_{AV}} + \rho_{AV} \sin(w_{AV}\ t) - k_{SA-AV}\, x_3 + k^t{}_{SA-AV}\, x_1{}^{\tau_{SA-AV}} - k_{HP-AV}\, x_3 + k^t{}_{HP-AV}\, x_5{}^{\tau_{HP-AV}}$$

$$\dot{x_5} = x_6$$

$$\dot{x_6} = -a_{HP}\, x_6\, (x_5 - w_{HP1})(x_5 - w_{HP2}) - \frac{x_5(x_5+d_{HP})(x_5+e_{HP})}{d_{HP} e_{HP}} + \rho_{HP} \sin(w_{HP}\ t) - k_{SA-HP}\, x_5 + k^t{}_{SA-HP}\, x_1{}^{\tau_{SA-HP}} - k_{AV-HP}\, x_5 + k^t{}_{AV-HP}\, x_3{}^{\tau_{AV-HP}} \tag{3.7}$$

In additions, Gois & Savi, proposed that the ECG signal is generated by the composition of individual signals of the oscillators, and that a linear combination of each oscillator signal can be described as follows:

ECG signal = $(\alpha_o+\alpha_1 x_1+\alpha_3 x_3+\alpha_5 x_5)$ similarly, $\frac{dECG}{dt} = \alpha_1 x_2+\alpha_3 x_4+\alpha_5 x_6$

Where,

- α_o , is a term that influences on the coupled final and α_1 , α_3 , α_5 are constants which influences terms for each oscillator at final ECG
- The pairs (x_1, x_2) , (x_2, x_3) & (x_4, x_5) show *SA, AV and HP oscillators* respectively
- a_{SA}, w_{SA1}, w_{SA2}, d_{SA}, e_{SA}, a_{AV}, w_{AV1}, w_{AV2}, d_{AV}, e_{AV}, a_{HP}, w_{HP1}, w_{HP2}, d_{HP}, e_{HP} model parameters
- k_{SA-AV} , $k^t{}_{SA-AV}$, k_{SA-HP} , $k^t{}_{SA-HP}$, k_{AV-SA} , $k^t{}_{AV-SA}$, k_{AV-HP} , $k^t{}_{AV-HP}$, k_{HP-SA} , $k^t{}_{HP-SA}$, k_{HP-SA}, $k^t{}_{HP-SA}$, are unidirectional coupling terms
- $x_i{}^{\tau}=x_i(t-\tau)$, τ is time delay which represents the time necessary for the transmission of signals between different parts of heart
- $\rho_{SA}\sin(w_{SA}\ t)$, $\rho_{AV}\sin(w_{AV}\ t)$ and $\rho_{HP}\sin(w_{HP}\ t)$ are external forcing terms

Currently, there are no well recognized mathematical models related to the activities of heartbeat. So, Zeeman nonlinear heartbeat model was used in this study because of its simplicity.

3.2. Zeeman Heartbeat Dynamics and Model Validation Analysis

There are two extreme conditions of equilibrium during the heartbeat cycle, namely diastole, which is the state of relaxation and systole which is the phase of contract. The presence of a pacemaker suited at the top of the atrium helps the heart to undergo beating. It allows the heart to contract into systole. In other words, it causes an electro-chemical pulse that gradually travels through the atria causing muscle fibers to contract and forces blood into the ventricles, so that expands quickly through the ventricles forcing the ventricle to contract and sends a massive blood pump down to arteries [26].

As Breitenstein pointed out [36], a good mathematical model which describes the heartbeat activity should contain three basic characteristics:

i. A stable equilibrium phase representing diastole;
ii. A threshold to activate the electrochemical wave that triggers the heart to reach the systole; and
iii. The rapid returning to diastolic state.

The original Zeeman model in equation 3.1 is used to perform the above criteria and the following parameter values have been taken for analysis.

Table 3.1: Parameters of the model [22] [23**]**

Parameter	x_d	ϵ	T	x_s
Value	1.024	0.2	1	-1.3804

For x_d = 0, the equilibrium point is at (0, 0).

$$A = \begin{bmatrix} \frac{-1}{\epsilon}(3{x_1}^3 - T) & \frac{-1}{\epsilon} \\ 1 & 0 \end{bmatrix}.$$ Where, A is the Jacobean matrix for equation (3.1).

A at equilibrium point (0, 0) can be defined as:

$$A = \begin{bmatrix} \frac{T}{\epsilon} & \frac{-1}{\epsilon} \\ 1 & 0 \end{bmatrix}$$

Since both eigenvalues A are positive i.e. 3.618 and 1.382, the origin is unstable.

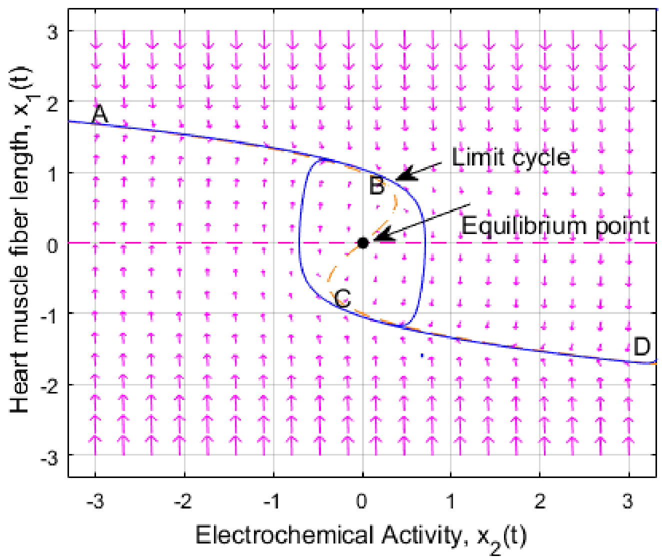

Figure 3.1: Phase portrait of heartbeat system for $\boldsymbol{\epsilon = 0.2}$, *T=1 and* $x_d = 0$

The phase portrait of equation (3.1) with the initial conditions is shown in figure 3.1. The dashed curve showed the steady state. Both trajectories end around its equilibrium point in the limit cycle. The equilibrium point is clearly unstable, because of vector field in the limit cycle points away from the equilibrium point. In figure 3.1, the vector field across the portion AB and CD often leads towards the dashed line, showing stable sections, whereas, points along the segment BC are unstable. Points B and C are essential as they define the threshold, satisfying the heartbeat model selection criteria (ii).

The eigenvalue is negative for $3x_1^2 - T > 0$. Therefore, the system model is stable if $x_1 \geq \sqrt{T/3}$ which belongs to the segment AB, and $x_1 \leq -\sqrt{T/3}$ which belongs to segment CD. Besides, the thresholds for triggering from diastolic to systolic states on point B i.e. $x_1 = \sqrt{T/3}$, and $x_1 = -\sqrt{T/3}$ on point C.

The diastole state can be calculated by varying value of x_d in such a way as to fulfill the above stabilization condition. The requirements will be met if the x_d is 1.024. Therefore, the stable equilibrium is at (1.024, –0.049) because of the eigenvalues are negative i.e. -0.48826 and -10.2404.

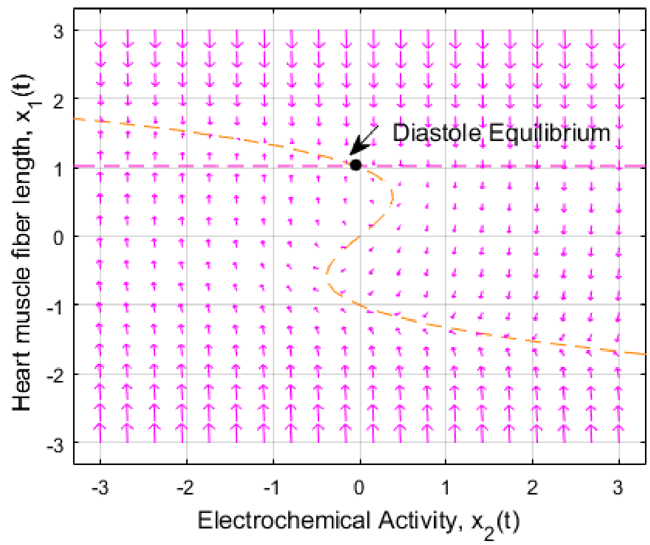

Figure 3.2: Phase portrait of heartbeat system during diastole for $\boldsymbol{\epsilon = 0.2}$, *T = 1 and* x_d = 1.024

The Figure 3.2 showed the system's phase portrait for x_d =1.024. The equilibrium point at (1.024,-0.0497) is stable and defines as the condition of diastole equilibrium, i.e. it satisfies the first characteristics I: a stable equilibrium. For this case, all trajectories go to the diastole equilibrium point independent of their primary conditions. The system remains indefinitely at the same point of equilibrium, other than an external excitation that causes the system to transfer to a new point of equilibrium. Depending on this new stable system (equation 3.2), the heartbeat model is combined with a control input in equation (3.8) as written below:

$$\varepsilon\dot{x}_1 = -\,(\,x_1{}^3 - Tx_1\, + x_2)$$

$$\dot{x_2}\ = (x_1 - x_d) + (x_d - x_s)\ \mathrm{u(t)},\ T\ >\ 0 \tag{3.8}$$

Another parameter is added, x_s describes average fiber length during the heart is at systolic state and *u(t)* defines the control mechanism of cardiac pacemaker which guides the heart in to the diastole and systolic states. The equilibrium state of the heartbeat system would be modified between the diastole and the systolic states by introducing pacemaker signal either on or off form.

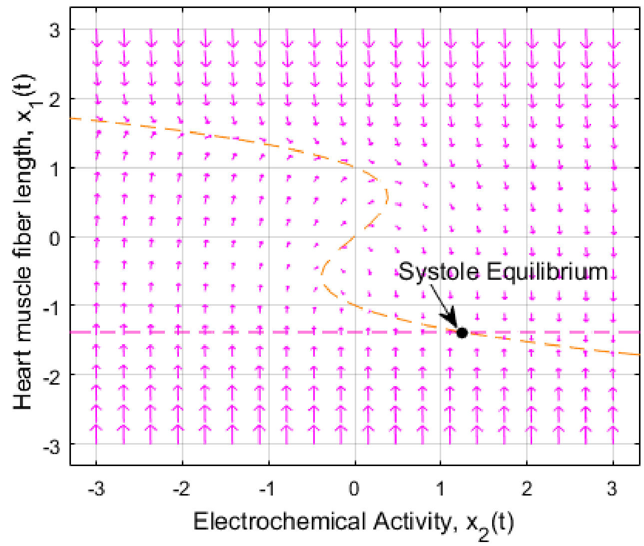

Figure 3.3: Phase portrait of heartbeat system during systole

The phase portrait plot when *u(t)* switched on with $x_s = -1.3804$ is shown in figure 3.2. At (-1.3804, 1.25), stable equilibrium point is obtained. Therefore, based on the control signal, the on off control strategy is effective in modeling the state transitions from diastole to systole (III satisfied).

The above three criteria's are expected from the physical behavior of heart. Hence, these validate the heartbeat model.

3.3. Considered Disturbances of Cardiovascular System

The brain regulates feeling, thought, motion and all functions. Scientists believe that there are one hundred billion neurons in a typical adult human brain and each neuron is linked to two hundred fifty thousand other neurons.

In comparison to skeleton muscles, which need to be simulated by the nervous system, heart can produce its own electrical stimulation. Interestingly, the heart can beat without brain orders, so it has to be adjusted in conditions where the brain determines the heart rhythm, such as (exercise, hormones such as epinephrine (adrenaline)) are emitted (often correlated with feelings such as apprehension, nervousness and excitement) (Amy Kuklev). The nervous system can allow the heart rate to go faster or slower, but cannot create it.

It is very normal for the brain waves to have a considerable impact on the heart rate and cardiovascular system, its function being disruption if overdosed. Brain waves are typically divided into four categories of frequency bands such as; Beta, Alpha, Delta, and Theta. Beta has high frequency band and small amplitude, while delta has low frequency band and high amplitude [37].

Table 3.2: Brain wave frequency bands [37]

Categories of brain wave taken as a disturbance		
BETA	(14-100Hz)	Arousal, Anxiety, disease, fight
ALPHA	(8-13.8Hz)	Pre-sleep, pre-walking, drowsiness
THETA	(4-7.9Hz)	Deep mediation, Hypnagogic
DELTA	(1-3.9Hz)	Loss of body awareness, Dreamless

3.4. Heart Rate Calculations and Reference ECG signal

To determine the heart rhythm, the ECG signal is measured using wavelet transforms' built in function. It can be determined using the following formula [38].

$$\text{Heart Rate} = \frac{60}{\text{R}-\text{R interval in seconds}}$$

The average heart beat for a healthy human is 72 bpm. Normal person heart rate is 60–100 bpm [38]. The actual signal in figure 3.4 was obtained from MIT-BIH physioNet database in the name of 16773m.mat. The data is described with irregular surges of high-frequency and severe noise in the lower channel having sample frequency 128Hz, and 1280 columns (samples/signal) [38]. To eliminate noise from the ECG data by high pass filtering, pre filtering was added. Then the ECG signal is squared to eliminate the negative and to be very clear or noticeable R-R peaks.

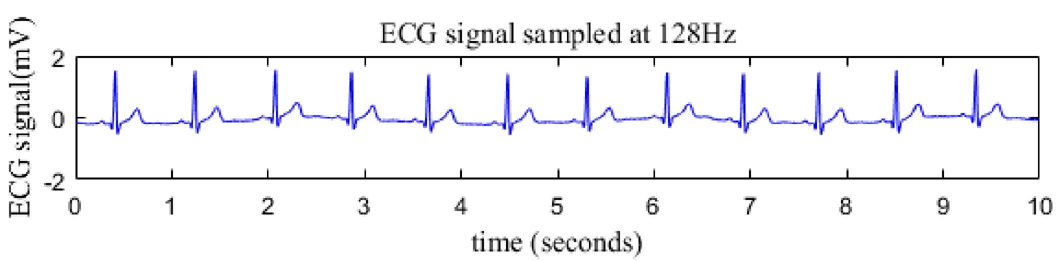

Figure 3.4: ECG data

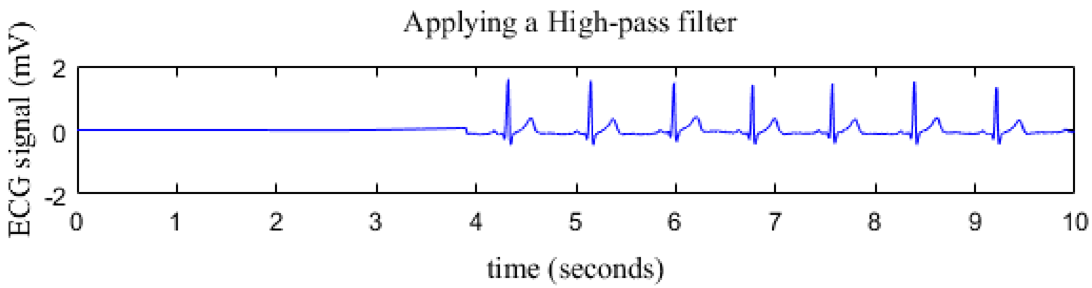

Figure 3.5: Filtered ECG signal

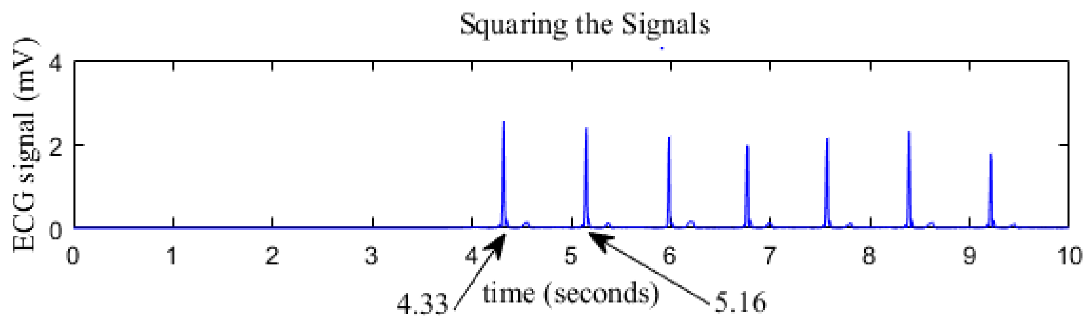

Figure 3.6: Squared ECG signal

From figure 3.6, the R-R peak interval is calculated as:

$$\Rightarrow 5.16 - 4.33 = 0.83\text{. Then, Heart Rate} = \frac{60}{0.83} \cong 72 \text{ bpm}$$

3.5. Controller Design

3.5.1. Introduction

There are different types of control methods that could be used for system control. Regular and abnormal dynamic behavior has been described in the analysis of nonlinearities, especially in biological systems, and it is different in any person. The behavior of biological system has been observed linearly for decades, which removes a wealth of information on the natural processes in question. The latest work indicates that certain cardiac arrhythmias display nonlinear feature usually associated with a disorderly response. The theory of nonlinear system and the chaos associated with biomedical system became scientific attention [39].

Nonlinear control methods are more common, and they can be used in both linear and nonlinear systems. These controllers can be extended from linear to nonlinear systems, solving various problems such as system uncertainties and resistance of external disturbance [40].

In 1977, Utkin proposed sliding mode control (SMC) in the international literature which had previously been established in Russia. The approach has many benefits such as low sensitivity to changes in system parameters, and robustness to external disturbances. In addition, the method's solution algorithm gives a systematic modeling process that reduces the specifications of the exact system model. The approach has been researched and applied extensively for both linear and nonlinear systems, multi input/multi output systems, and discrete-time and large-scale systems [41].

The major reasons for selecting this controller in wide range is having acceptable control efficiency and solve two major demanding control topics with exceptional precision, robustness, and simple tuning and implementation [42]. This controller, though, is used in a wide variety, but the pure sliding mode controller has the following drawbacks. Frist, chattering problem, which may cause the output of controller to oscillate at high frequency. Secondly, sensitivity; if the input signal is very close to zero, this system is very sensitive to noise [42].

Chattering phenomena can cause certain problems for electronic pacemaker components, such as saturation and heat. To minimize or remove the chattering, several researchers did different studies and grouped them into two main methods, namely the method of boundary layer saturation and estimated method of uncertainties [41] [42].

Some authors conducted fuzzy logic technique in sliding mode controllers (FSMC) to minimize chattering problems happened in the use of SMC and other researchers implemented sliding mode technique with fuzzy logic controller (SMFLC) to improve system stability which is the most significant challenge in pure FLC [42]. The discussion in this thesis is restricted to the more popular fuzzy sliding mode control (FSMC).

3.5.2. Design of Sliding Mode Controller

The first phase of the SMC design allows a custom made sliding surface to be designed. The plant dynamics on the sliding surface are limited to surface equation and are stable to handle plant uncertainties and external disruption. In the second stage, a feedback control law is needed to provide to convergence of a system trajectory hits the surface in a finite time (reaching mode) beginning from any initial state, and then slides along the surface to the target (sliding mode) [41][43][44].

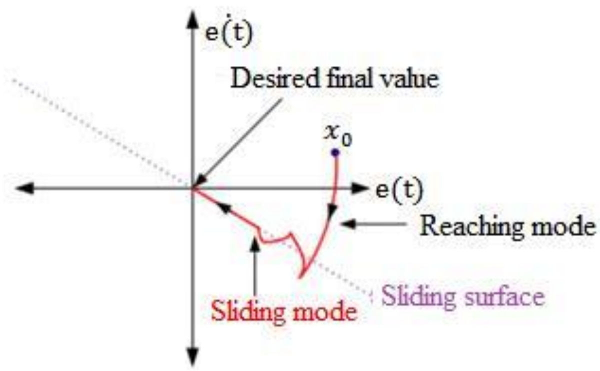

Figure 3.7: Graphical explanation of SMC [44]

As defined above, it is functional for controlling the nonlinear heartbeat model according to the features and properties of this controller.

2nd order heartbeat model in equation (3.8) is considered to design a control signal, by letting $y(t) = x_2(t)$ as output measurement (measured as potential across muscle fiber) and y_r(t) as desired signal. The tracking error rate and its rate of change are defined as:

$$e = y_r - y \tag{3.9}$$

$$\dot{e} = \dot{y}_r - \dot{y} \tag{3.10}$$

The objective is to enforce $e(t) \rightarrow 0$ such that $y(t) \rightarrow y_r$ (t) as $t \rightarrow \infty$. The heartbeat model correlated with disturbance is defined as;

$$\begin{aligned} \varepsilon\dot{x}_1 &= -\left(x_1{}^3 - Tx_1 + x_2 \right) \\ \dot{x}_2 &= (x_1 - x_d) + (x_d - x_s)\,u(t) + d(t) \end{aligned} \tag{3.11}$$

Equation (3.11) is a nonlinear function and has uncertainty. Additionally, the $d(t)$ assumed to be a system disturbance. The following assumptions are required in order to design the control input.

a. System states are observable.
b. $d(t)$ is unknown, however, constrained, i.e. $d(t) < D$. Where, the positive constant of $|D|$ is known.
c. The control rule is based on the ECG signal

First, the sliding surface, called the switching function, is selected as follows:

$$s(e,t) = s(t) = \lambda e(t) + \int_0^t e(\tau)\,d\tau \tag{3.12}$$

Where, $e = y_r - y$, $\dot{e} = \dot{y}_r - \dot{y}$ $and\ \lambda$ is design parameter, which is the slope of sliding line selected to ensure the asymptotic stability of the sliding mode. The expression ($\int_0^t e(\tau)\, d\tau$) in equation (3.12) is added for the control input to appear when $s(e,t)$ is differentiated once.

The control method in SMC is the sum of two control laws: switching and equivalent control. In a finite time, the switching control enforces the system states to the specified sliding surface. Using the equivalent control rule obtained from the sliding function, the closed loop system will become insensitive to any parameter changes, and robust to matched disturbances [41].

SMC structure, therefore, comprises of switching and equivalent control as defined in equation (3.13) below.

$$u_{smc}(t) = u_{eq}(t) + u_{sw}(t) \tag{3.13}$$

Where, u_{sw} (t) represents switching control that involved when $s(e,t) \neq 0$, corresponds to the reaching phase. And, u_{eq} (t) the equivalent control corresponds to sliding phase when $s(e,t) = 0$.

The equivalent control, $u_{eq}(t)$, is derived by solving the first derivative of the sliding function i.e. $\dot{s}(e,t) = 0$, at every $t > t_o$ for some t_o , so it is obtained as:

$$\dot{s}(e,t) = 0.$$

$$\lambda\, \dot{e(t)} + e(t) = 0 \tag{3.14}$$

Substituting equation (3.11) in equation (3.14) yields the equivalent control as:

$$\lambda[\, \dot{y}_r - [(x_1 - x_d) + (x_d - x_s)u(t) + \mathrm{d}(\mathrm{t})]] + e(t) = 0$$

$$\Rightarrow\ u_{eq}(t) = \frac{1}{(x_d - x_s)}[\, \dot{y}_r - (x_1 - x_d) - \mathrm{d}(\mathrm{t}) + \frac{1}{\lambda}e] \tag{3.15}$$

And, u_{sw} is designed to minimize the interferences caused by time varying parameters or external disturbances to ensure system motion in sliding mode [45]. It is designed as:

$$u_{sw} = ksign(s(t)) \tag{3.16}$$

Where, $sgn(s)$ is a sign function, defined as: $sign(s) = \begin{cases} 1 & \text{if } s > 0 \\ -1 & \text{if } s < 0 \end{cases}$

Hence, the control signal, $u(t)$, is obtained by combining the above two equations, the continuous control function $u_{eq}(t)$ and the discontinuous control function $u_{sw}(t)$ of SMC, as follows:

$$u(t) = \frac{1}{(x_d - x_s)}[\, \dot{y}_r - (x_1 - x_d) - \mathrm{d}(\mathrm{t}) + \frac{1}{\lambda}e] + ksign(s(t)) \tag{3.17}$$

3.5.3. Stability Analysis

Lyapunov function is considered for analyzing the stability of the system and defined as;

$$V = \frac{1}{2}s^2 \tag{3.18}$$

It guarantees that the system state trajectory directs towards the switching surface on either side of *s(e,t)* = 0. The system defined in equations 3.17 is stable if and only if the derivative of the Lyapunov function is negative.

$$\Rightarrow \dot{V} < 0 \tag{3.19}$$

$$\Rightarrow s\dot{s} < 0s$$

$$\Rightarrow s\,\{\lambda\,\dot{e} + e\} < 0$$

$$\Rightarrow s\,\{\lambda[\dot{y}_r - (x_1 - x_d) - (x_d - x_s)\mathrm{u(t)} - \mathrm{d(t)}] + e\,\} < 0$$

By substituting the combined controller at $u(t) = u_{eq} + u_{sw}$, it gives as;

$$\Rightarrow s\{\lambda[\dot{y}_r - (x_1 - x_d) - (x_d - x_s)[\frac{1}{(x_d - x_s)}[\,\dot{y}_r - (x_1 - x_d) - \mathrm{d(t)} + \frac{1}{\lambda}e] + ksign(s(t))] - d(t)] + e\,\} < 0$$

$$\Rightarrow s\,\{-\frac{\lambda ksign(s(t))}{(x_d - x_s)}\} < 0$$

$$\Rightarrow s\,\{-\lambda ksign\big(s(t)\big)\} < 0 \tag{3.20}$$

Since $x_d = 1.024$ *and* $x_s = -1.3804$, the difference is positive constant. Therefore, to have a stable system the switching gain k and slope λ should be positive constants.

Using sign function in the SMC in equation 3.17 can induce high frequency trajectory chattering around the sliding surface and leading to system output oscillation around the reference values [46].

A boundary layer is added along with the switching surface to solve this issue and the sign function can be substituted by a saturation function sat(s/Φ) [46]. The selection of Φ is essential; the chattering problem cannot be overcome by small values of Φ and high values can increase the steady state error [46], requiring a compromise option when choosing the thickness of the boundary layer. In other words, if the switch gain is too high, then greater chatter will be produced. The control mechanism would be unstable if the switch gain is too low.

3.5.4. Design of Fuzzy Sliding Mode Controller

The combination of FLC with SMC is another way to reduce chattering phenomenon [46]. Therefore, in this thesis, a new Fuzzy Sliding Mode (FSMC) controller is used to control the nonlinear heartbeat model with SMC robustness and FLC smoothness. Figure 3.8 demonstrates the switching function of SMC and FSMC schemes. In this strategy, a fuzzy interference method substitutes the saturation function to smoothen the control operation. The overall block diagram of the fuzzy sliding mode control with the heartbeat system is shown in Figure 3.9 below.

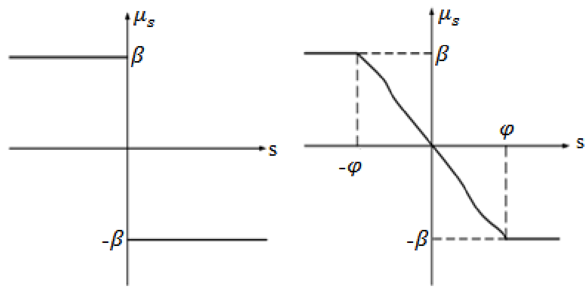

Figure 3.8: Switching function; sliding mode (a) and fuzzy sliding mode (b) [46]

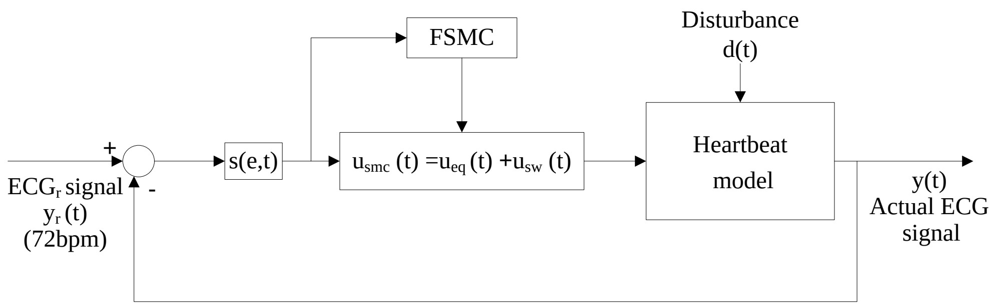

Figure 3.9: Design of fuzzy sliding mode control system of heartbeat model

Referring to the controller output of equations (3.17), fuzzy logic control is introduced in to SMC. The chattering mechanisms could be eliminated by developing acceptable control rules by fuzzy reasoning and fuzzy logic control as a regulatory tool for switching control. The output of FSMC is modified as:

$$u(t) = u_{eq}(t) + k_{fuzzy}\, u_{fuzzy}(t) \tag{3.21}$$

Where, u_{fuzzy} is the output of fuzzy logic control, and k_{fuzzy} is output gain of fuzzy logic

There are three major phases of the fuzzy logic controller. Namely; fuzzification, rule evaluation, and defuzzifcation [47].

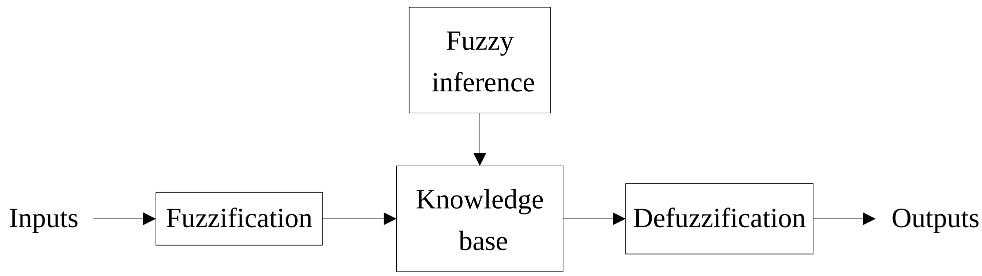

Figure 3.10: Concept of fuzzy logic controller

Fuzzification

It is described as an act of obtaining an input variable value (e.g. e(t)) and finding the membership function's numeric values specified for variables [48]. For simplicity, the sliding surface, *s(e,t)*, in this thesis is fuzzfied using seven triangular membership functions.

Rule Estimation (Knowledge Base)

The control rules should be designed in the way that state's trajectory bends into and slides cross the sliding surface on the phase plane in order to meet the conditions of existence. The Mamdani fuzzy inference approach has been used in this thesis to evaluate the fuzzy rule. There is one input (sliding surface) and one output (u_{fuzzy}) for the proposed FLC. Thereby, the fuzzy sets (linguistic variables) of the input and the output are defined, respectively as:

$$s = \{NB\ NM\ NS\ Z\ PS\ PM\ PB\} \qquad u_{fuzzy} = \{NB\ NM\ NS\ Z\ PS\ PM\ PB\}$$

Where, NB represents negative big, NM is represented for negative medium, NS is for negative small, Z is zero, PS is for positive small, PM is for positive medium and PB is for positive big.

The input is normalized at [−1, 1] interval, and the output is normalized at [−1, 1] interval. A set of decision rules in table 3.3 below is used to define the control scheme. The control input has seven fuzzy sets and 7 fuzzy rules. It solves the problem of fuzzy rule complexity.

Table 3.3: Fuzzy rule of FSMC

s(e,t)	NB	NM	NS	Z	PS	PM	PB
u_{fuzzy}	NB	NM	NS	Z	PS	PM	PB

The fuzzy universe of input *s* and output u_{fuzzy} are defined, and the membership functions are shown in figure (3.11) and (3.12), respectively as:

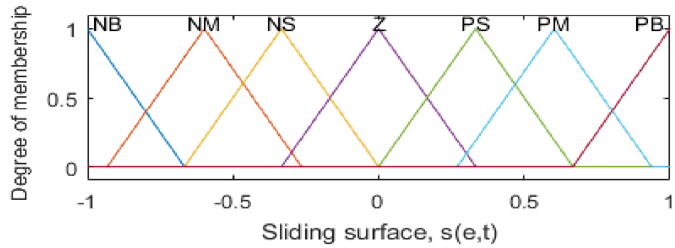

Figure 3.11: Input membership function of FSMC

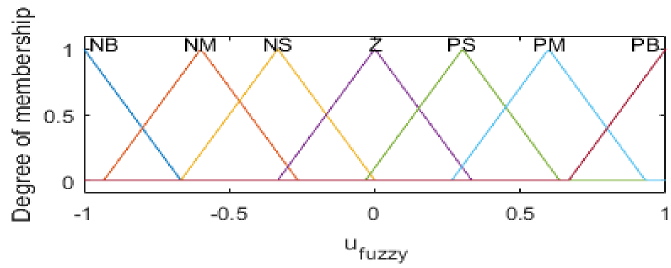

Figure 3.12: Output membership functions of FSMC

Fuzzy inference is therefore a method of translating membership values from the input to output, through the rule base. Finally, transformation after inference, defuzzification should also be implemented to evaluate fuzzy logic set numerical values of u_{fuzzy}.

Defuzzification

It is the procedure for mapping from a set of inferred fuzzy control signals contained within a fuzzy output window to a non-fuzzy (crisp) control. The Center of Gravity (COG) algorithm is also used to perform the method of defuzzification and can be expressed as;

$$\text{Crisp control signal} = \frac{\text{sum of first moment of area}}{\text{sum of areas}}$$

For continuous system equation (3.22)

$$u_{fuzzy} = \frac{\int u_{\mu(u)du}}{\int \mu(u)du} \tag{3.22}$$

Control surface of u_{fuzzy} in figure (3.13) below is shown.

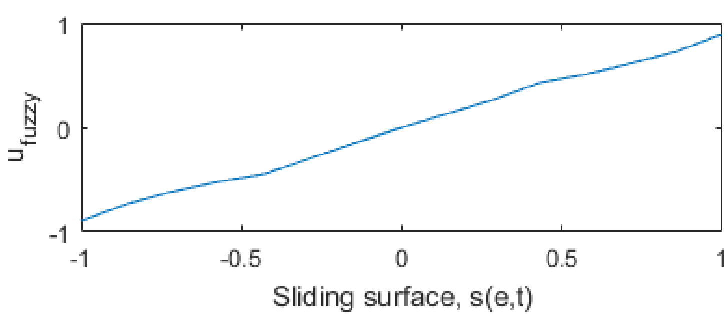

Figure 3.13: Control signal surface of FSMC

Chapter 4

Simulation Results and Discussions

4.1. Introduction

Simulation is carried out using Matlab®/Simulink®. The validity of heartbeat model was analyzed in chapter three. The overall combined system is shown in Figure 4.1. Second order of Zeeman heartbeat model has been used to perform simulation of the proposed controller to track real ECG data.

The tracking comparison performance of FSMC and SMC in terms of eliminating chattering was tested. In addition, the robustness of the proposed controller was tested on disturbance rejection, insensitive to parameter variations and time delay attack in sensed system.

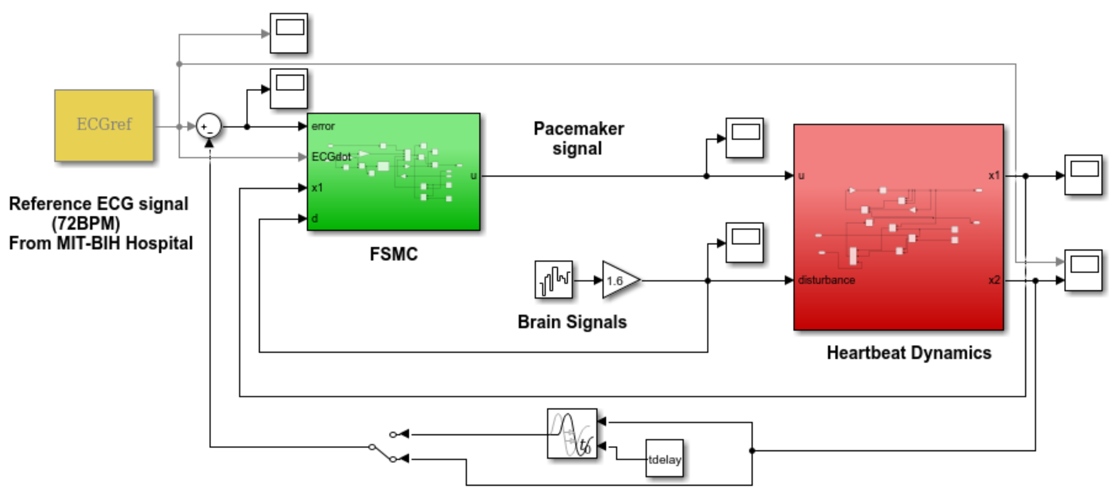

Figure 4.1: Simulink realization of FSMC for Zeeman heartbeat model

In this thesis, the parameters of the controller were tuned manually by looking the best tracking response of heartbeat system. The average healthy heartbeat for adult human (72 bpm) obtained from PhysioNet database was used as a reference signal and the simulation was explained in chapter three.

Table 4.1: Designed parameters of the controller

Controller	Values	
SMC	$\lambda = 1.7$	$k = 9$
FSMC	$\lambda = 1.7$	$k = 9$

The disturbance of electrical stimulation of heart with a noise (like, anxiety, disease) coming from human brain was considered system disturbance.

Table 4.2: Values of the Brain Frequency [37]

	Value
Wave Form	Random
Amplitude	20
Brain Frequency(Anxiety, disease)	100Hz

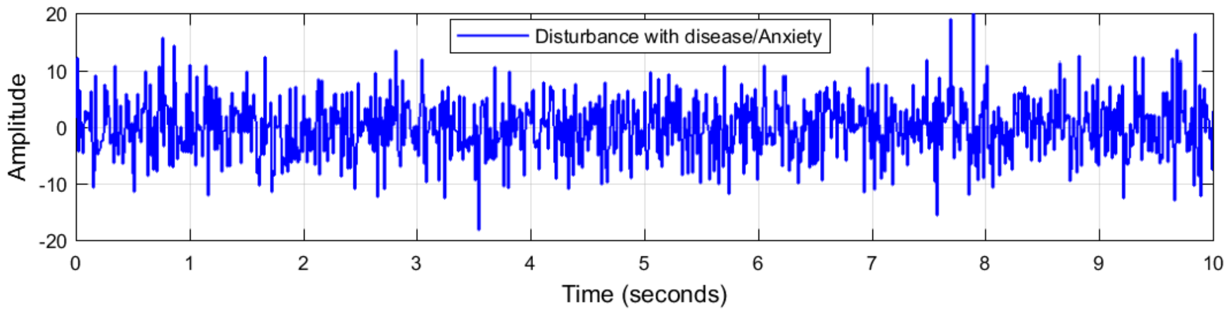

Figure 4.2: Disturbance signal

4.2. The Results

4.2.1. Performance Comparison of the System with SMC and FSMC

The simulation result with SMC shown in figure 4.3 below indicated that the output measurement $x_2(t)$ tracks the ECG signal from PhysioNet database and rejects external disturbance. Figure 4.4 and 4.5 also showed that there is too much chattering in pacemaker signal $u(t)$ and sliding surface $s(e,t)$, respectively.

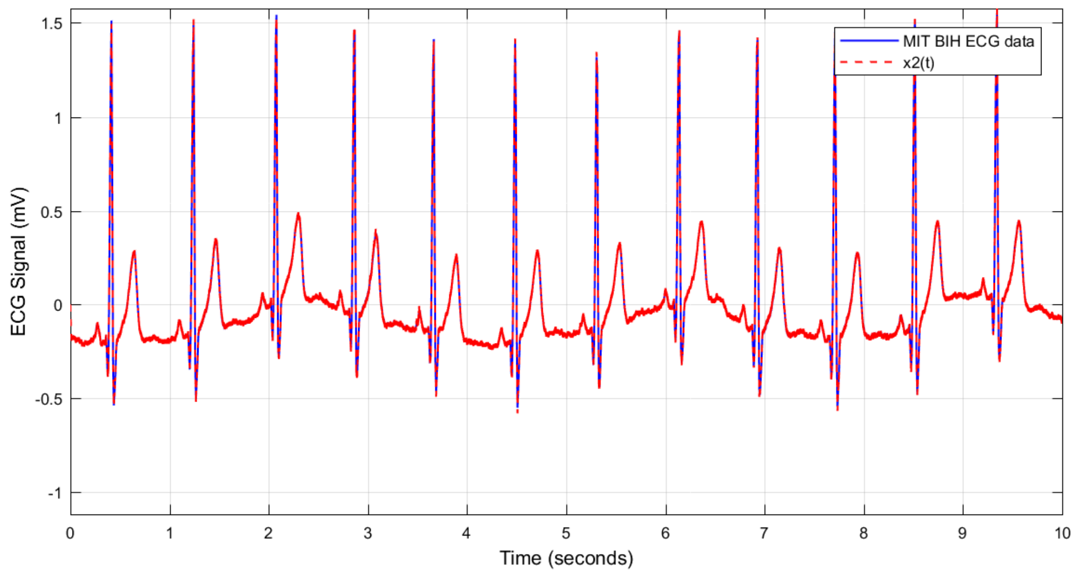

Figure 4.3: ECG signal tracking of SMC for heartbeat system with disturbance

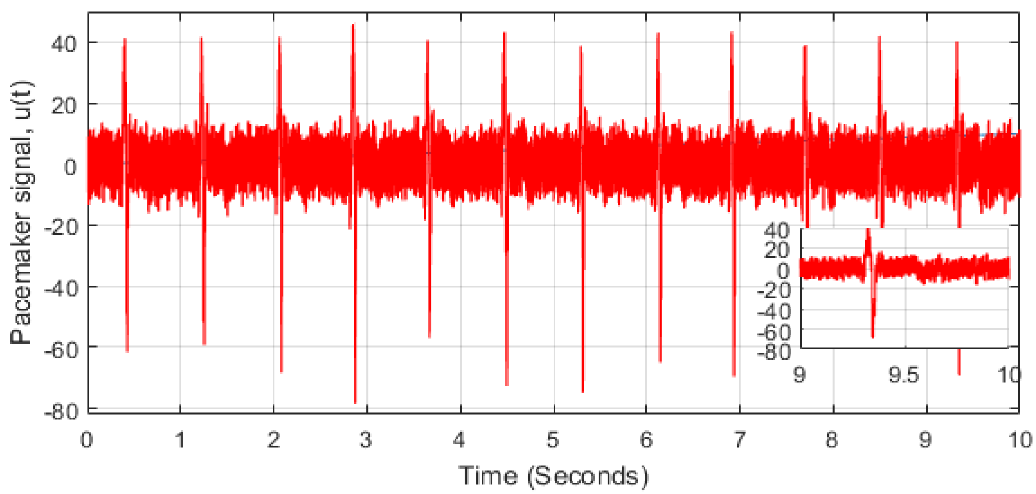

Figure 4.4: Pacemaker signal for heartbeat system with SMC

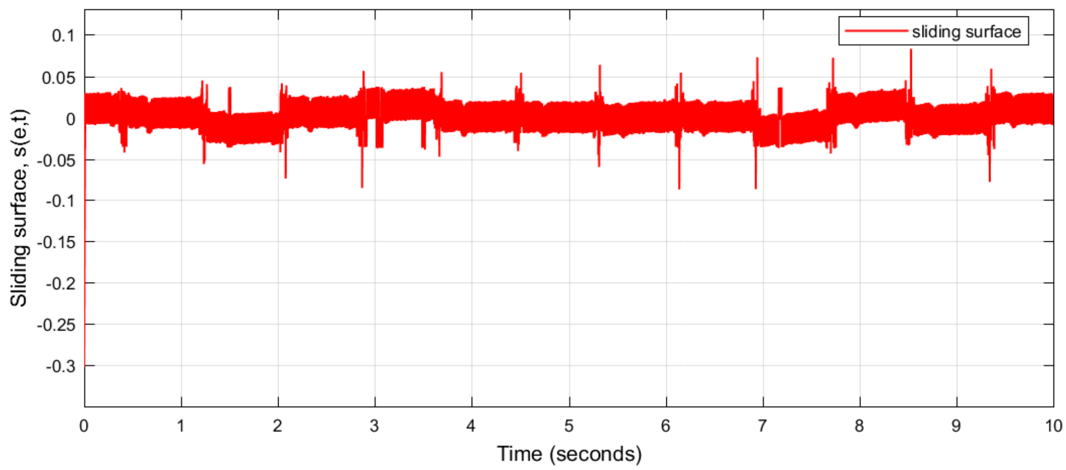

Figure 4.5: Sliding surface for heartbeat system with SMC

The result in figure 4.6 below showed the tracking performance of FSMC. It rejects external disturbance. The simulation result also showed that the FSMC is superior to SMC in eliminating chattering phenomenon which appeared in the pacemaker signal as it is seen in figure 4.7 and 4.8.

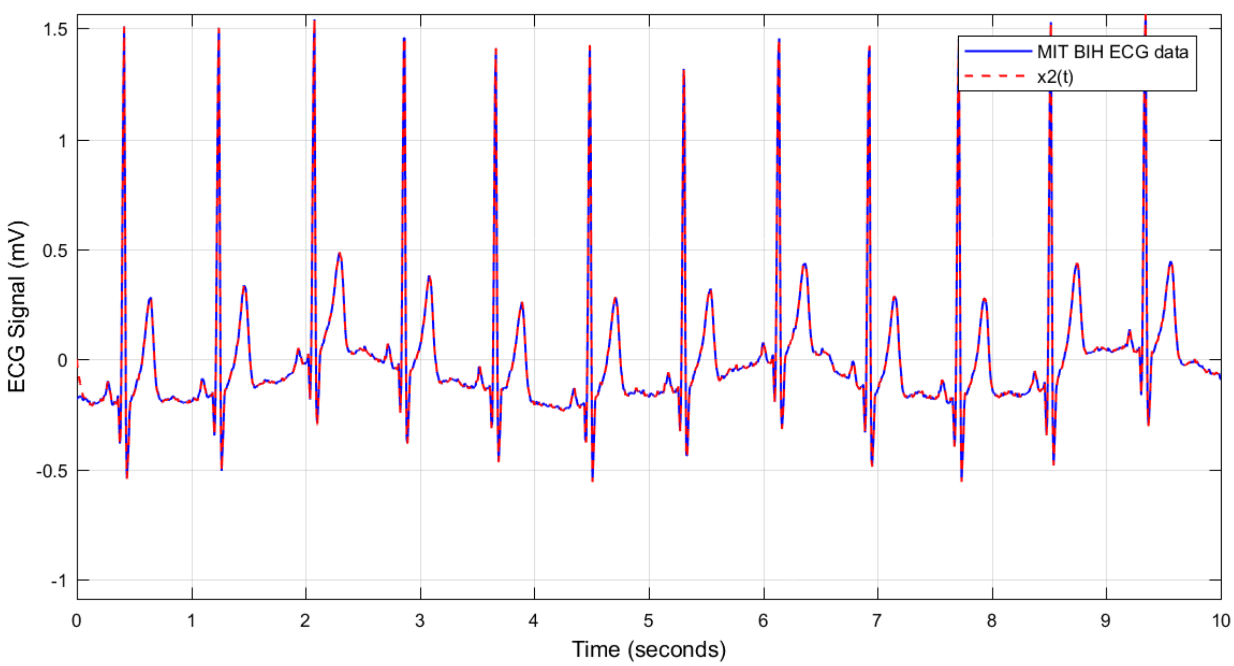

Figure 4.6: ECG signal tracking of FSMC for heartbeat system with disturbance

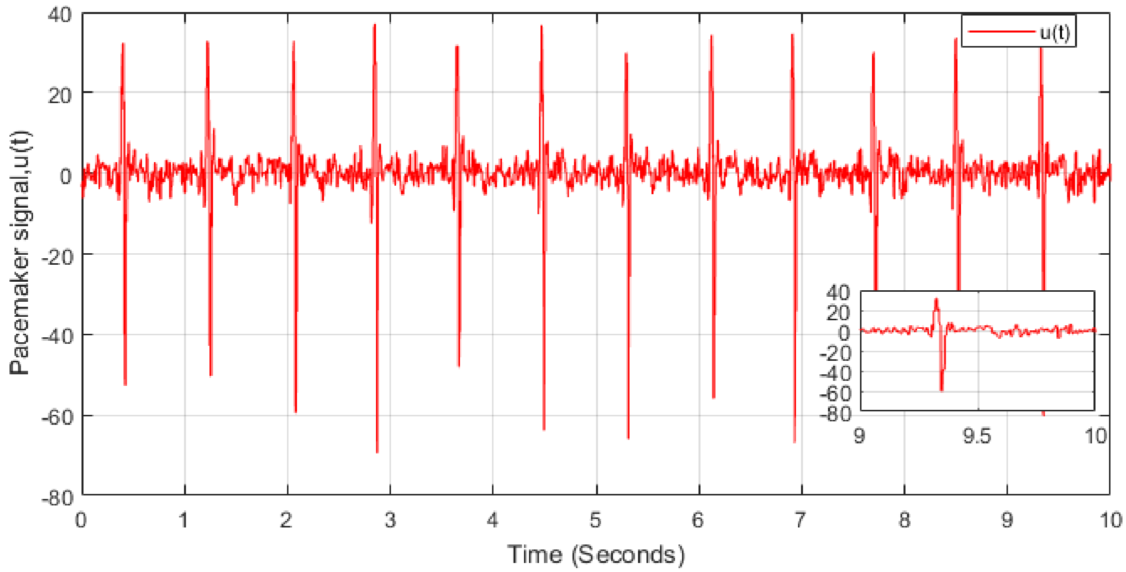

Figure 4.7: Pacemaker signal for heartbeat system with FSMC

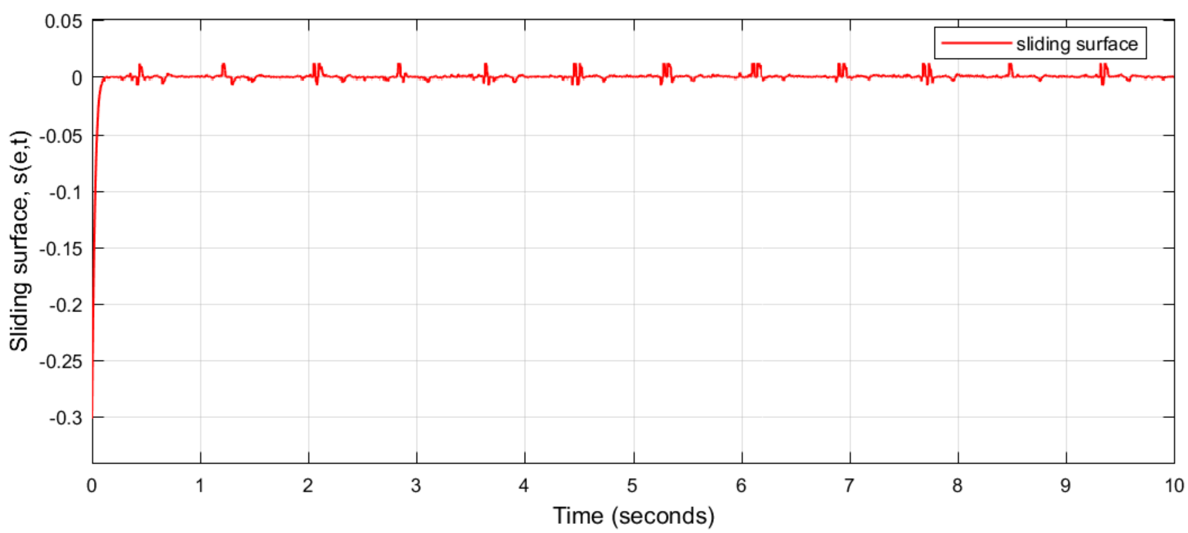

Figure 4.8: Sliding surface of FSMC for heartbeat system

Table 4.3: Comparison of controller performance

Performance comparison criteria	Controller algorithms	
	SMC	FSMC
Mean square error	0.000337	0.000104
Root mean square error	0.01228	0.007234
Pacemaker signal at fundamental frequency	3.343peak (2.293 rms)	2.163peak (1.529 rms)
THD	168.4%	47.05%

From FFT window, the amplitude of the real ECG data from MIT BIH was 0.00307 peak, ECG generated using FSMC was 0.0246 peak, and ECG generated using SMC was 0.06642 peak. Therefore, the generated ECG signal using FSMC was closer to Real ECG data.

The figure 4.9 below showed the system trajectory of the resting of muscle fiber length $x_1(t)$ in the heart. It is maximum during relaxing and minimum during contraction states of heartbeat system.

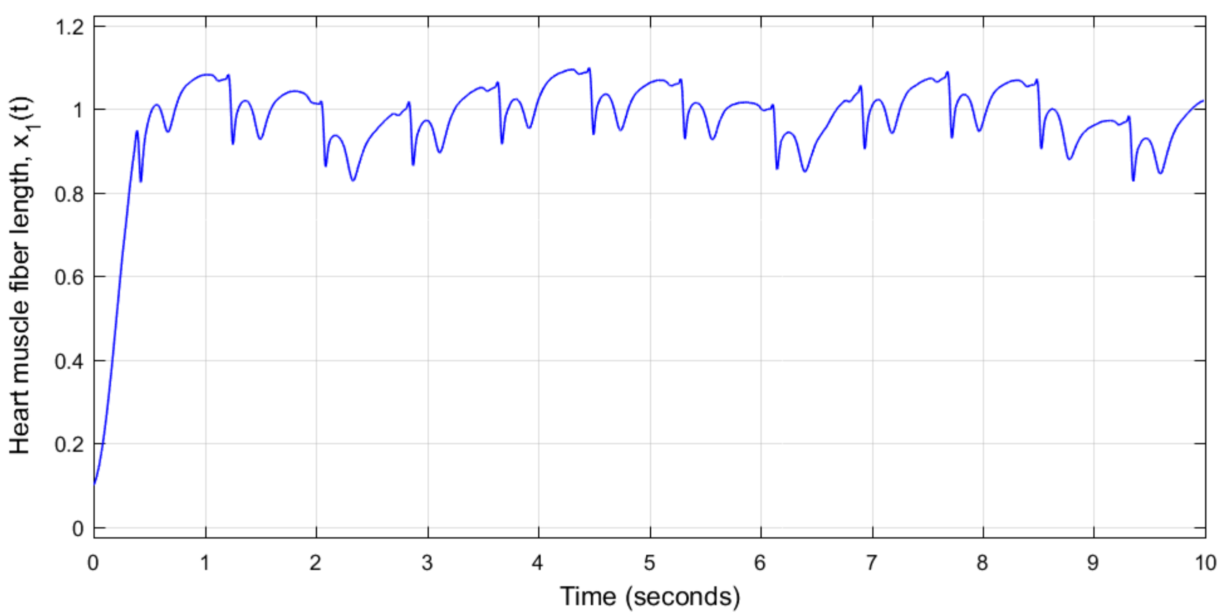

Figure 4.9: Simulation result of $x_1(t)$ for heartbeat system

4.2.2. Result of the System with FSMC at External Disturbance and Parameter Variations

The performance of controller was tested for heartbeat system using different values of muscle tension related to blood pressure at $T=1$ (low blood pressure), and $T=10$ (high blood pressure). In addition, to show the effect of parameter uncertainties, the system is simulated at different values for heartbeat system. Thus, the figure 4.10 and 4.11 showed that better tracking of real ECG signal by the proposed controller under parameter variations and disturbances. This assured that the FSMC is robust system.

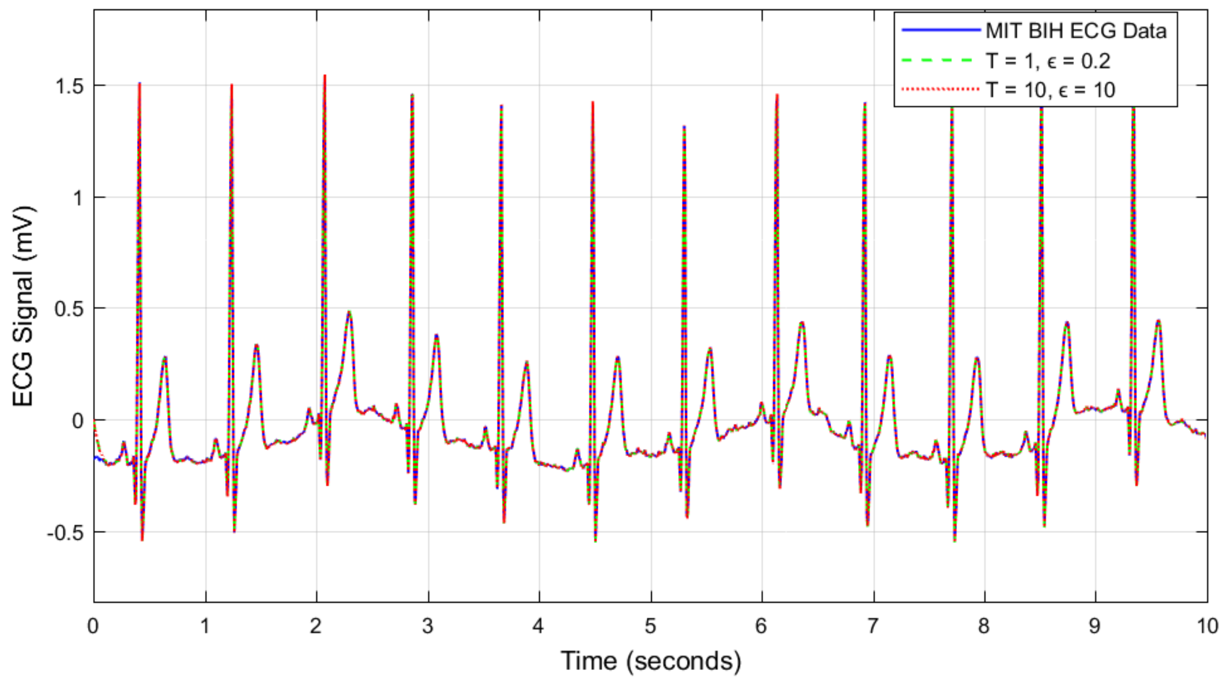

Figure 4.10: ECG signal tracking of FSMC for heartbeat system at different values of T and ϵ

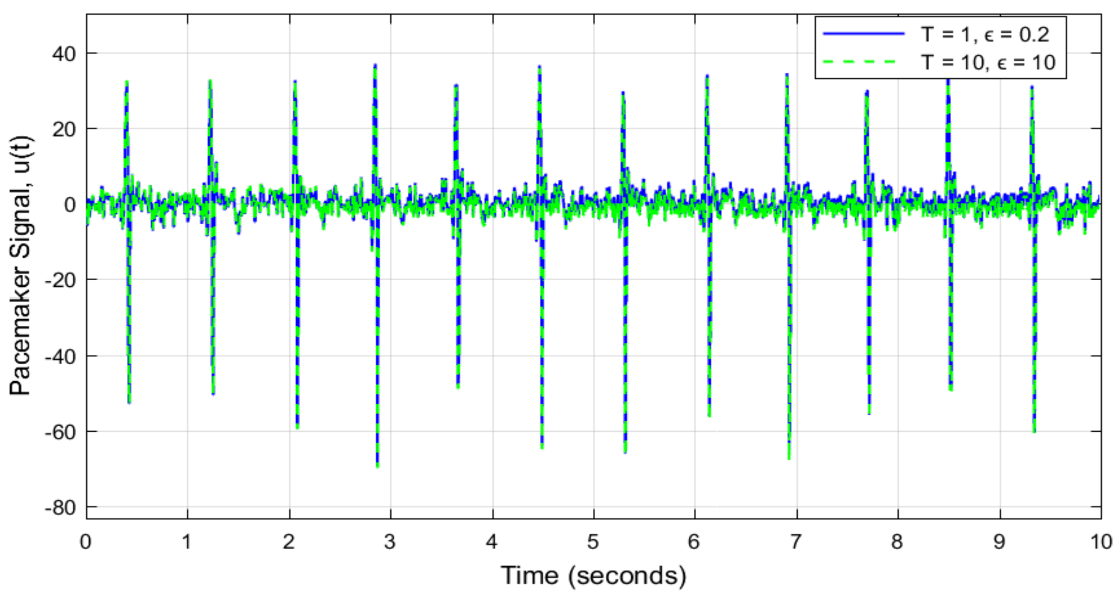

Figure 4.11: Simulation result of $u(t)$ of heartbeat system for different values of T and ϵ

4.2.3. Result of the System with FSMC under Time Delay Attack at the Sensed Loop and Disturbance

In addition, the performance of FSMC was tested when random feedback time delay was introduced on heartbeat sensing system with time delay $\tau = 0.01$ sec. The figures 4.12 showed that the FSMC tracks the reference signal accurately for heartbeat system.

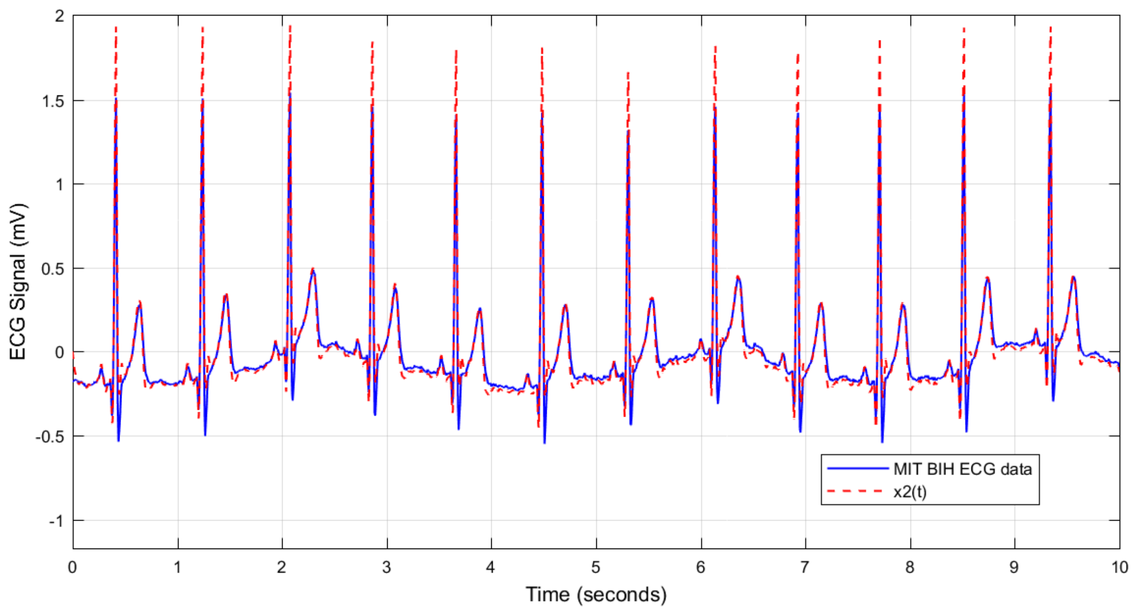

Figure 4.12: ECG signal tracking of FSMC for heartbeat system under time delay attack and disturbance

Chapter 5

Conclusions and Future Works

5.1. Conclusions

In this thesis, fuzzy sliding mode controller was applied to heartbeat system which can track the real healthy ECG signal. Several cardiac related mathematical models associated with the heartbeat were studied and Zeeman model was selected. The model validation was tasted by using the Breitenstein principle.

The average heart rate (72 bpm) used for reference signal was calculated from the ECG signal pattern in terms of beat per minute by finding the interval between two consecutive R waves. In addition to this, the brain signal can indirectly affect the heart electrical conduction activity. The BETA type brain signals like anxiety, disease were considered as a disturbance.

The design of proposed controller stability was proved using Lyapunov function. In order to compare the performance of the controller developed by FSMC with SMC, different evaluation conditions have been selected. The robustness of FSMC to control Zeeman heart model with bounded disturbance, parameter perturbation and feedback time delay attack were demonstrated.

It is seen that both SMC and FSMC applied to Zeeman heart model were able to track ECG data obtained from physioNet database accurately under bounded disturbance with asymptotic stable error. The chattering observed in SMC result was eliminated, the total harmonic distortion analyzed from FFT window was reduced by 121.35% and root mean square error was also reduced by 0.00005% while using FSMC which will be used in the practical design of controller for pacemakers.

Furthermore, the simulation results obtained show that high robustness of FSMC in the presence of parameter variations for different blood pressure or other parameters of the heartbeat model.

Finally, the robustness of FSMC controlling Zeeman heartbeat model in feedback time delay attack was also demonstrated and found to be a robust system.

5.2. Future Works

Even if successful result was obtained based on the control objective, there are other several ways where this research can also be improved in the future. Some of those are mentioned below:

- Heartbeat model used in this thesis is based on the Sino-atrial (SA) node pace making, dominant pacemaker compared with the lower one produced by Atrial-ventricular (AV). In the future, researchers can use coupled VDP oscillator models at AV node and His purkinjie system to make pace making better.
- Muscle fiber length and electrochemical property of heart is not the same for different individuals and may be changed by human health conditions, emotions and brain signals. The recent research focuses on the average adult. Thus, adding more considerations of patient condition can be studied in the future.
- In this thesis, the controller parameters were tuned manually. Appropriate optimization algorithm may be applied to get better results in the future. In addition, the pacemaker controller can be done for different body conditions of the patient such as walking, running and other cases need to be studied for temperature or environmental changes.
- Other versions of sliding mode controller such as twisting, super twisting, higher order SMC …, and other nonlinear control techniques will be studied in the future.

References

[1]. Zia Farooq, Salman Ahmad, "Bifurcation Analysis of Heartbeat Model", *Journal of Space Technology*, Vol 7, No 1, July 2017

[2]. Kirkwood G, Fox DJ, Brown BD. "Bradycardia pacing", *Medicine*. 2014: pp.615-619.

[3]. N. Kannathal, et. al., "Cardiac state diagnosis using adaptive neuro-fuzzy technique", *Medical Engineering & Physics*, Vol. 28, 2006, pp. 809-815

[4]. WHO.WHO Africa Region: Ethiopia, Non Communicable disease. 2014

[5]. Shi WV, Zhou M., "Optimal single-pulse for pacemakers based on a sino atrial model", *IEEE/ASME Transactions on Mechatronics*, 2013; 18(1):348-54

[6]. Shi, W.V. and Zhou, M.C., "Body Sensors Applied in Pacemakers", *A Survey*. *IEEE Sensors Journal*, 2012, 1817- 1827

[7]. Shi, W.V. and Zhou, M.C, "Design Fuzzy PID Controllers for Dual-Sensor Pacing Systems in Patients with Bradycardia at Rest", *IEEE International Conference on Systems, Man, and Cybernetics (SMC)*, Anchorage, 9-12 October 2011, pp.1117-1122

[8]. M Holzer and W Behringer, "Therapeutic hypothermia after cardiac arrest," *Curr. Opin. Anaesthesiol.*, vol. 18, pp. 163–168, 2005.

[9]. Mohamed Esmail Karar, "Robust RBF neural network–based back stepping controller for implantable cardiac pacemakers", *Int J Adapt Control Signal Process,* 2018.*pp.*1040–*1051*.

[10]. Siroos Nazari, et. al., "A New Three-Oscillator Model for the Heart System in the Case of Time Delay and Designing Appropriate Controller for Its Synchronization", *Hindawi Publishing Corporation ISRN Applied Mathematics,* Volume 2014, Article ID 168247.

[11]. Thomas Leti, et. al., "Interest of analyses of heart rate variability in the prevention of fatigue states in senior runners", *Elsevier, Conference Paper* · January 2009.

[12]. Arthur C. Guyton, et. al., "*Text book of Medical Physiology"*, Eleventh Edition.

[13]. Andrew, T. Resiner, et. al., "The physiological basis of the Electrocardiogram", Biomedical Signal and Image Processing, spring 2007

[14]. N. Jafarnia-dabanloo, et. al., "a modified Zeeman model for producing HRV signals and its application to ECG signal generation," *journal of theoretical biology*, vol. 244, no. 2, 2007, pp. 180-189.

[15]. S.A.P. Haddad, et. al., "The evolution of pacemaker", IEEE Engineering in Medicine and Biology Magazine, vol.25, 2006, pp. 38-48

[16]. Srnmo, P.Laguna, “Bioelectrical Signal Processing in Cardiac and Neurological Applications”, vol. 1, *Academic Press*, 2005.

[17]. D.L. Hayes and P. A. Friedman, “Cardiac Pacing, Defibrillation and Resynchronization”, *A Clinical Approach*. New York: Wiley, 2008.

[18]. S. Petrutiu, et. al., “High resolution electrocardiography optimized for recording pulses from electronic pacemakers: Evaluation of a new pacemaker sensing system,” *Comput. Cardiol*, vol. 34, pp. 197–200, 2007.

[19]. H. Karam E. et. al., “Design of Model Free Sliding Mode Controller based on BBO Algorithm for Heart Rate Pacemaker” *I.J. Modern Education and Computer Science,* 2019, 3, 31-37

[20]. M. J. Lopez, et. al., “Computer Simulation and Method for Heart Rhythm Control Based on ECG Signal Reference Tracking,” *WSEAS Transactions on Systems*, Vol. 9, No. 3, 2010, pp.263-272.

[21]. W. Thanom and R. N. K. Loh, “Nonlinear Control of Heartbeat Models,” *Journal on Systemics, Cybernetics and Informatics*, Vol. 9, No. 1, 2011, pp

[22]. W. Thanom and R. N. K. Loh, “Observer-Based Nonlinear Feedback Controls for Heartbeat ECG Tracking Systems,” *Journal on Intelligent Control and Automatio*n, Vol. 3, No. 1, 2012, pp 251-26.

[23]. Arman Sargolzaei, et.al., “Control of Nonlinear Heartbeat Models under Time Delay-Switched Feedback Using Emotional Learning Control,” *Int. J. on Recent Trends in Engineering and Technology*, Vol. 10, No. 2, Jan 2014:

[24]. Ferreira, B.B., et. al., “Chaos Control of the Cardiovascular Dynamics,” *22nd International Congress of Mechanical Engineering* (COBEM 2013)

[25]. S. Behnia and J. Ziaei, “A New Dynamical Control Scheme to Control of Abnormal Synthetic ECG Signals”, *Chaotic Modeling and Simulation (CMSIM)* 3: 281-289, 2016.

[26]. E. C. Zeeman, "Differential equations for the heartbeat and nerve impulse", *in Dynamical Systems, Elsevier*, 1973, pp. 683-741.

[27]. Noble D., “A modification of the Hodgkin-Huxley equations applicable to Purkinje fiber action and pacemaker potentials”, *The Journal of Physiology*. 1962; 160(2):317-52.

[28]. P. N. Tu, “Dynamical systems: an introduction with applications in economics and biology”, *Springer Science & Business Media*, 2012.

[29]. D. S. Jones and b. D. Sleeman, “differential equations and mathematical biology,” *chapman & hall/crc*, London, 2003.

[30]. N. Jafarnia-dabanloo, et. al., “a modified Zeeman model for producing hrv signals and its application to ecg signal generation,” *journal of theoretical biology*, vol. 244, no. 2, 2007, pp. 180-189.

[31]. Van Der Pol B, “On relaxation oscillation”, *Philosophical Magazine*. 1926: pp.978-992.

[32]. B. Van der pole and j. Van der mark, “the heart beat considered as a relaxation oscillation and an electrical model of the heart,” *philosophical magazine series* 7, vol. 6, no. 38, 1928, pp. 763-775.

[33]. Santos, et. al., “Rhythm synchronization and chaotic modulation of coupled Van der Pol oscillators in a model for the heartbeat”, *Physica* A. 2004; 335- 355.

[34]. Grudzinski K and Zebrowski JJ, “Modeling cardiac pacemakers with relaxation oscillators”, *Physica A*. 2004; 336:153-162.

[35]. S. R. Gois and M. A. Savi, “An analysis of heart rhythm dynamics using a three coupled oscillator model,” *Chaos, Solitons & Fractals*, vol. 41, no. 5, pp. 2553–2565, 2009.

[36]. S. Breitenstein, “Cardiovascular modeling: The mathematical expression of blood circulation”, *Master's thesis, University of Pittsburgh*, PA, 1993

[37]. M.Aabid, A.Elakkary N.Sefiani, “stabilization of human heart using pid controller”, *Journal of Theoretical and Applied Information Technology*, October 2016. Vol.92. No.1.

[38]. Ledisi G. Kabari, et. al., “Bradycardia Detection using ECG Signal Processing and MATLAB”, *EJERS, European Journal of Engineering Research and Science,* Vol. 4, No. 3, March *2019*.

[39]. Felipe Rebelo Lopes and Jorge Audrin Morgado de Gois, “ECG model parameters optimization and space state reconstruction”, *Journal of the Brazilian Society of Mechanical Sciences and Engineering*, 2018.

[40]. C. Edwards and S. K. Spurgeon, “Sliding Mode Control: Theory and Applications”, Taylor and Francis, 1998.

[41]. Murat Furat *and* Ilyas Eker, “Chattering-eliminated adaptive sliding-mode control: an experimental comparison study”, *Turk J Elec Eng & Comp Sci* (2016) 24: pp.605 – 620.

[42]. Farzin Piltan and Nasri B. Sulaiman, “Review of Sliding Mode Control of Robotic Manipulator”, *World Applied Sciences Journal*, 2012. pp. 1855-1869.

[43]. J. Y, Hung, et. al., "Variable Structure Control: A Survey", *IEEE Trans. on Industrial Electronics*, vol. 40, No. 1, Feb. 1993.

[44]. G.Sivaramakrishna, Dr. R. Vijaya Santhi, "Design of Adaptive Sliding Mode Control with Fuzzy Controller and PID Tuning for Uncertain Systems", IRJET, Volume: 04 Issue: 09 | Sep -2017.

[45]. Shi Yfeng, et. al., "Fuzzy Sliding mode controller for the swing arm used in a Fourier transform spectrometer", *information technology journal*, pp. 736-747, 2011.

[46]. J. Lo and Y. Kuo, "Decoupled Fuzzy Sliding Mode Control," *IEEE Trans. Fuzzy Syst.*, Vol.6, No. 3, Aug. 1998, pp. 426-435.

[47]. M.A.A.Morsy, et. al., "Design and Implementation of Fuzzy Sliding Mode Controller for Switched Reluctance Motor", *Proceedings of the International Multi Conference of Engineers and Computer Scientists* 2008 Vol II IMECS 2008.

[48]. Jens Jakel, et. al., "Fuzzy control systems", *control systems, robotics and automation*-vol. XVII.

Appendix

Appendix A: Detailed Simulink representation of the system

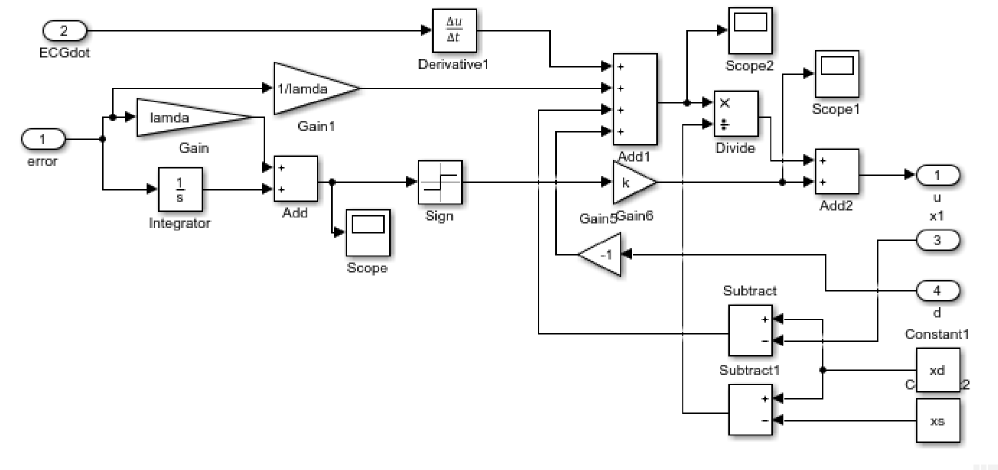

Figure A.1: Realization of SMC for heartbeat system

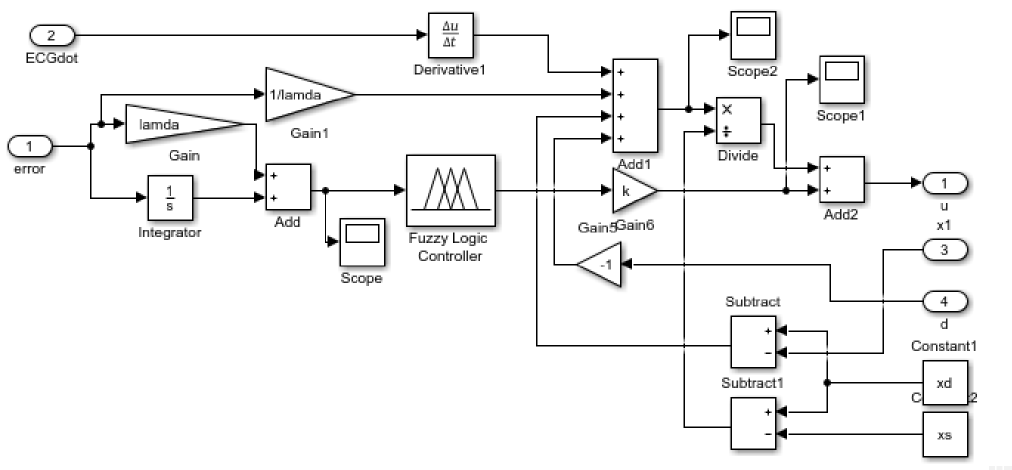

Figure A.2: Realization of FSMC for heartbeat system

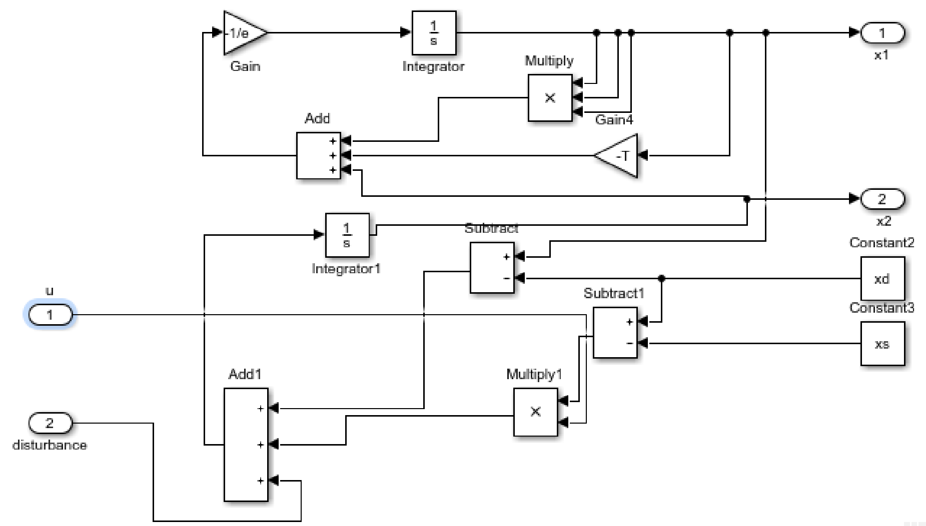

Figure A.3: Realization of heartbeat system

Appendix B: Rule viewer of fuzzy inference

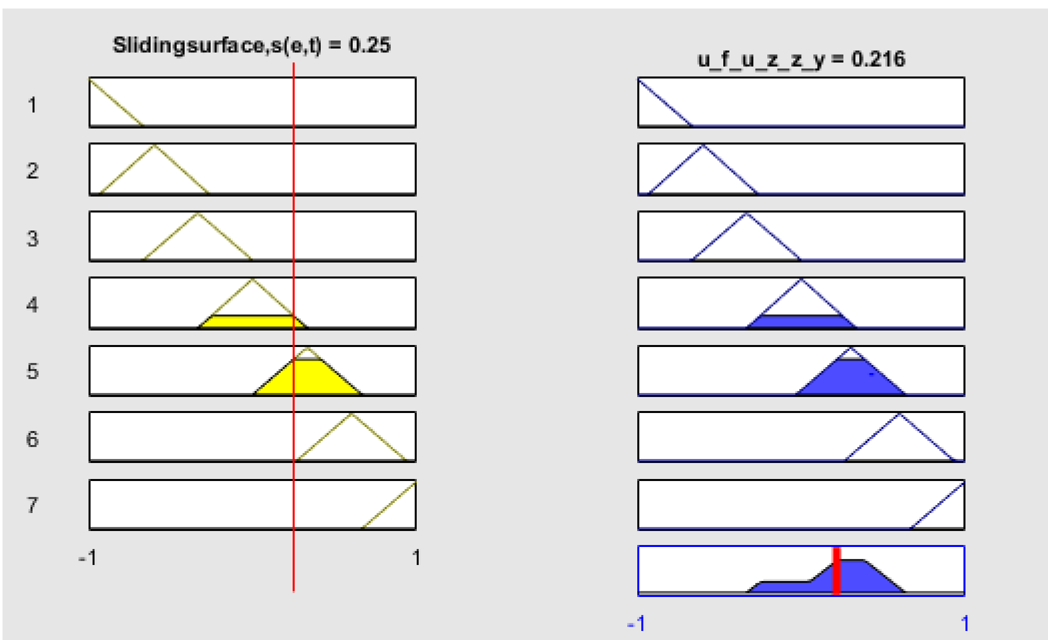

Appendix C: pplane 8.m was used to draw the phase portraits plot of heart beat system

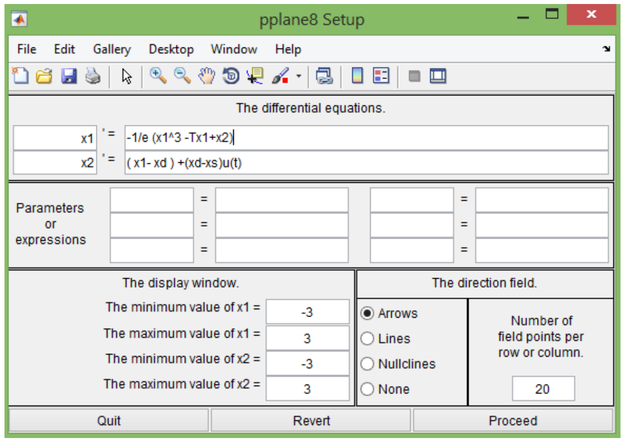

Appendix D: MATLAB code for Generating ECG signal From PhysioNet database and constants

```
% © Anteneh Nebyu, 2020
% Adress: anenehnebyu@gmail.com
load ('16773m.mat'); % load val signal and 16773m is  heartbeat id for a person
valu=transpose(val);
Esignal= (valu-0)/400;% 0 is for base and 400 is for gain
Fs=128; % sampling freq in Hz
t =(0:length(Esignal)-1)/Fs;% time is 1/Fs
time=transpose(t);
ECGref=[time Esignal];
subplot(3,1,1);
plot(t,Esignal);
xlabel('time (seconds)');
ylabel('ECG signal (mV)');
title('ECG signal sampled at 128Hz');
% when high pass filter is applied
hf=fir1(1000,1/360*2,'high');
Esignal_filter = filter(hf,1,Esignal);
subplot(3,1,2);
plot(t,Esignal_filter);
xlabel('time (seconds)');
ylabel('ECG signal(mV)');
title('a High-pass filter applied ');
% when the signal is squared
desqr=(Esignal_filter.^2);
subplot(3,1,3);
plot(t,desqr);
xlabel('time (seconds)');
ylabel('ECG signal (mV)');
title('when the Signal is squared ');
xd=1.024; % muscle fiber length during diastole
T=1; % muscle tension at low blood pressure
T1=10; % muscle tension at high blood pressure
e=0.2; % e and e1 fast eigenvalues of the system
e1=10;
xs=-1.3804; % muscle fiber length during systole state
lamda =1.538; % sliding surface slope
kfuzzy = 9; % output gain of fuzzy logic
tdelay=0.01; % time delay in seconds
```